C. R. Palevol 18 (2019) 72–89

Contents lists available at ScienceDirect

Comptes Rendus Palevol

www.sciencedirect.com

Human Palaeontology and Prehistory (Palaeoanthropology)

Enamel and dentine dimensions of the Pleistocene hominins from Atapuerca (Burgos, Spain): A comparative study of canine teeth

Proportions d'émail et de dentine des dents des hominines pléistocènes d'Atapuerca (Burgos, Espagne) : étude comparative des canines

Cecilia García-Campos[a,b,*], María Martinón-Torres[a,b], Laura Martín-Francés[a,c], Mario Modesto-Mata[a,b], Marina Martínez de Pinillos[a,d], Juan Luis Arsuaga[e], José María Bermúdez de Castro[a,b]

[a] *Centro Nacional de Investigación sobre la Evolución Humana, Paseo de la Sierra de Atapuerca 3, 09002 Burgos, Spain*
[b] *Anthropology Department, University College London, 14 Taviton Street, WC1H 0BW London, UK*
[c] *Université de Bordeaux, UMR 5199 PACEA, 33615 Pessac cedex, France*
[d] *Laboratorio de Evolución Humana, Departamento de Historia, Geografía y Comunicación, Universidad de Burgos,Plaza de Misael Bañuelos s/n, 09001 Burgos, Spain*
[e] *Centro Mixto UCM-ISCIII de Evolución y Comportamiento Humanos, Madrid, Spain*

ARTICLE INFO

Article history:
Received 27 April 2018
Accepted after revision 27 June 2018
Available online 30 November 2018

Handled by Roberto Macchiarelli

Keywords:
Atapuerca
Canines
Dentine
Enamel
Microcomputed tomography

Mots clés :
Atapuerca
Canines
Dentine
Email
Microtomographie

ABSTRACT

Enamel and dentin patterns have awakened a considerable interest in phylogenetic studies. However, almost nothing is known about the dental tissue proportions of European Pleistocene hominins, apart from Neanderthal populations. This study aims to assess the three-dimensional dental tissue proportions of permanent canines belonging to the extensive sample of hominin teeth at Sierra de Atapuerca (Spain) through the use of microtomographic techniques. Our results show that early and middle Pleistocene populations from Atapuerca exhibit large coronal and root dentine dimensions, as well as a thinly enamelled pattern, which has been traditionally considered an autapomorphic Neanderthal trait. Therefore, these results might support an early enamel thickness decrease which is already observed 800 kyr ago in *Homo antecessor* and maintained in later groups such as Sima de los Huesos and Neanderthal populations during the middle Pleistocene.

RÉSUMÉ

Les patrons de proportions de l'émail et de la dentine ont éveillé un intérêt considérable dans les études phylogénétiques. Cependant, on ne connaît encore presque rien sur les proportions des tissus dentaires des hominidés du Pléistocène européen, à l'exception de celles des populations néandertaliennes. La présente étude vise à évaluer les proportions tridimensionnelles des tissus dentaires des canines permanentes issues d'un échantillon exceptionnel de dents d'homininés d'Atapuerca (Espagne)

* Corresponding author. Centro Nacional de Investigación sobre la Evolución Humana, Paseo de la Sierra de Atapuerca 3, 09002 Burgos, Spain.
E-mail address: ceciliagc.bio@gmail.com (C. García-Campos).

https://doi.org/10.1016/j.crpv.2018.06.004
1631-0683/

en utilisant des techniques microtomographiques. Nos résultats montrent que les populations du Pléistocène moyen et inférieur d'Atapuerca possèdent des proportions de dentine radiculaire et coronaire élevées, ainsi qu'un patron d'émail fin qui a été traditionnellement considéré comme un caractère autapomorphique des Néandertaliens. Par conséquent, ces résultats appuient l'apparition précoce d'une diminution de l'épaisseur de l'émail depuis au moins 800 ka chez *Homo antecessor*. Ce patron d'émail fin est également observé dans d'autres groupes plus tardifs, tels que Sima de los Huesos et les populations néandertaliennes pendant le Pléistocène moyen.

1. Introduction

Dental traits are considered to be highly heritable, selectively neutral and evolutionary conservative (Rathmann et al., 2017; Scott and Turner, 2000). Accordingly, teeth can be considered as a true 'black box' of the genetic code, whose morphology reflects the result of the interaction between phylogenetic heritage and the selection for functional adaptations. Therefore, they are a source of information about the life history, diet, taxonomy and behaviour of extant and extinct hominin species (Grine, 2005; Kono, 2004; Martin, 1983; Martin et al., 2003; Olejniczak et al., 2007; Schwartz, 2000; Smith et al., 2005, 2008), thus representing a useful tool in taxonomic and phylogenetic studies.

Tooth tissues, in general, and enamel thickness, in particular, have been of considerable interest over the past century. Most of the available data for the interpretation of dental tissue variability in human evolution come from studies about the enamel thickness of posterior dentition (Grine, 2002, 2005; Kono and Suwa, 2008; Kono et al., 2002; Olejniczak et al., 2008a; Skinner et al., 2015). Researches based on both controlled plane sections and volumetric data of molars enabled to successfully distinguish relatively thinly enamelled extant African apes from thickly-enamelled hominin taxa, including modern humans (Grine and Martin, 1988; Kono, 2004; Martin, 1985; Olejniczak et al., 2008b; Smith et al., 2005, 2006; Tafforeau, 2004). On the other hand, reports on naturally-fractured molars belonging to African early *Homo* (Beynon and Wood, 1986; Ramirez Rozzi, 1998) and Asian *H. erectus* (Smith et al., 2009) showed that these species had thinner cuspal enamel than the more robust *Australopithecus* (Beynon and Wood, 1986; Ramirez Rozzi, 1998), allowing one to appreciate a tendency towards thickness decrease.

Besides early *Homo*, studies on broader samples also showed a tendency towards enamel thickness decrease in later *Homo*, including Neanderthals, fossil *H. sapiens* and modern humans (Olejniczak et al., 2008a; Smith et al., 2012). However, such changes occurred in a different way in the two lineages. Studies on postcanine tissue proportions showed that Neanderthal populations and modern humans have absolutely similar amounts of enamel (Olejniczak et al., 2008a; Smith et al., 2012). Nevertheless, it has been observed that, in the case of *H. neanderthalensis*, the enamel is deposited over a more complex and larger EDJ surface associated with a higher dentine-pulp complex dimension, thus leading to a slightly lower enamel thickness compared to that of modern humans (Olejniczak et al., 2008a; Smith et al., 2012). In fact, thinly enameled tooth crown has been identified as one of the autapomorphic Neanderthal features (Bayle et al., 2009a; Olejniczak et al., 2008b; Smith et al., 2012).

Therefore, comparative evidence suggests that the transition from early to middle Pleistocene gave rise to the emergence of two tendencies in the postcanine dental tissue pattern in the subsequent populations. Whereas African *H. erectus*/*ergaster* shows the intermediate-thick enamel condition (Smith et al., 2012; Zanolli, 2014) similar to that later observed in *H. neanderthalensis* (Olejniczak et al., 2008a), a relatively and absolutely thicker enamel is systematically found in Indonesian *H. erectus* and in fossil and extant modern humans (Smith et al., 2012; Zanolli and Mazurier, 2013; Zanolli, 2014; Zanolli et al., 2014, 2018).

In contrast to the posterior dentition, tissue proportions of the anterior teeth have been barely studied (Bayle et al., 2017; Buti et al., 2017; Feeney et al., 2010; Le Cabec et al., 2012, 2013; Saunders et al., 2007; Schwartz and Dean, 2005; Smith et al., 2008, 2012; Zanolli et al., 2014). Following Martin's pioneering work (1983, 1985), some studies have assessed 2D enamel thickness of the canine teeth through the use of a single physical cross section (e.g., Feeney et al., 2010; Saunders et al., 2007; Schwartz and Dean, 2005; Smith et al., 2008, 2012). Among them, the only study in which the variation of this trait has been investigated within the human fossil record is that carried out by Smith et al. (2012). They found that, whereas early *Homo* canines show substantial variations, the enamel thickness trends in later species' anterior teeth were largely paralleled to those observed for the molars. More recently, Buti et al. (2017) carried out an extensive study based on microtomographic techniques in which they investigated 3D enamel thickness variation in a sample comprising both Neanderthal and modern human upper and lower permanent canines. Before this work, only the study carried out by Bayle et al. (2017) on Neanderthal specimens from Sima de las Palomas del Cabezo Gordo (Spain) had provided information about the permanent canine enamel volume. The results obtained by these authors agreed with previous findings: Neanderthal canines have significantly lower relative enamel thickness values than typical in recent humans. Additionally, the comparison of dental tissue proportions between Neanderthal and late Pleistocene *H. sapiens* deciduous teeth has produced consistent evidence that supports the results obtained for the permanent

dentition (Bayle et al., 2009a, 2009b, 2010, 2017; Benazzi et al., 2011).

Despite such research work, the variation in dental tissue proportions within the genus *Homo*, and in particular the origin of the two enamel thickness tendencies that appeared in Neanderthals and modern humans is poorly understood. This is mainly due to the absolute scarcity of data on early European populations. Moreover, the European Pleistocene fossil record is principally composed of isolated and geographically-dispersed remains of diverse chronologies, which complicates the evaluation of the different evolutionary scenarios.

In this context, large tooth samples of well-defined populations, such as those of the archaeological complex collections from Sierra de Atapuerca in Spain, could contribute to fill this gap. On the one hand, the Gran Dolina sample is composed of the earliest human remains documented so far in western Europe. The mosaic of primitive and derived features characterising this group gave rise to the new species *H. antecessor* (Bermúdez de Castro et al., 1997) and has triggered a debate about its relationship with the Neanderthal and *H. sapiens* lineages (Bermúdez de Castro et al., 1997, 2003, 2015, 2017). On the other hand, the human fossil collection from Sima de los Huesos has become the most representative sample for the middle Pleistocene worldwide, which stands for more than 80% of the human fossil record for this period (Bischoff et al., 2003). This population is characterized by a combination of primitive traits (plesiomorphies) not found in later Neanderthals, by incipient Neanderthal-like traits (mesomorphies), and by typical Neanderthal traits (apomorphies), which suggest a close relationship with the Neanderthal lineage (Arsuaga et al., 1997).

This study aims to increase the amount of information currently available on dental tissue proportions of early European *Homo* species. To do so, microtomographic (micro-CT) imaging analytical techniques have been applied to the hominin tooth samples from the early and middle Pleistocene Atapuerca sites (Burgos). Then, the enamel and dentine volumes (Olejniczak et al., 2008a) and surfaces (Skinner et al., 2008a, 2008b) of a sample of permanent canine teeth belonging to these populations have been measured. Our objective is to discuss the meaning of the possible similarities and differences of Gran Dolina and Sima de los Huesos samples with the *H. neanderthalensis* remains of Krapina (Croatia) as well as with a recent modern human sample from Europe and Africa. In particular, with the present study we intended to test the following hypotheses. First, the dental tissue proportions of Krapina remains are similar to those published in literature in which broader *H. neanderthalensis* samples have been employed (Buti et al., 2017). Second, given the presence of an important number of apomorphic traits typical from Neanderthals in Sima de los Huesos population, the differences in dental tissue patterns between both populations are not significant. Third, given the chronological distance with the other populations examined and that most of their dental traits are primitive, Gran Dolina canine teeth conserve the pleisiomorphic thickly-enamelled pattern. And fourth, as the enamel thickness is not homogeneously distributed in the crown dental wear affects the taxonomic comparisons.

2. Materials and methods

2.1 Materials

The tooth assemblage from the Sierra de Atapuerca archaeological complex (Table 1) consists of three permanent canines (two upper and one lower) from the early Pleistocene Gran Dolina (TD6) site and 32 permanent canines (16 upper and 16 lower) from the middle Pleistocene Sima de los Huesos (SH) site. A detailed description of the sample studied here can be found below. The lithostratigraphic and geochronological contexts of the sites are described in detail in the Appendix 1.

At least 160 human fossil remains belonging to *H. antecessor* were recovered from the Gran Dolina level TD6-2, recently assigned to MIS 21 through different geochronological techniques applied to samples from TD7 and TD6 (Arnold et al., 2014; Berger et al., 2008; Falguères et al., 1999; Moreno et al., 2015). Based on direct ESR dating of a hominin tooth, the last published results indicate a time range from 772 to 949 kyr (Duval et al., 2018). The TD6 hominins show a certain number of derived features also present in middle Pleistocene and early Late Pleistocene populations (Bermúdez de Castro et al., 2013). In particular, the relatively high number of features exclusively shared with Neanderthals and with the Atapuerca-SH hominins are noteworthy (Bermúdez de Castro et al., 2013, 2015). As mentioned, this mosaic of characteristics supported the definition of the new taxon *H. antecessor* (Bermúdez de Castro et al., 1997; Carbonell et al., 1995) and has originated a debate about its relationships with the last common ancestor of Neanderthals and modern humans (Bermúdez de Castro et al., 1997, 2003, 2015, 2017). The three *H. antecessor* canines used in this study show a good preservation state. Specifically, ATD6-1 presents a slight cervical erosion, which nonetheless does not affect the enamel, and the ATD6-69 root had not finished forming.

The middle Pleistocene sample of Sima de los Huesos consists of 16 upper and 16 lower permanent canines. The human remains from this site are represented in a single lithostratigraphic level (LU6) (Arsuaga et al., 2014), which has provided mean ages of 433 ± 15 kyr and 416 ± 12 kyr using post-infrared-stimulated luminescence (pIR-IR) and thermally transferred optically stimulated luminescence (TT-OSL), respectively (Arnold et al., 2014). Initially, this human group was assigned to *H. heidelbergensis* (Arsuaga, 1993; Arsuaga et al., 1991, 1997; Bermúdez de Castro et al., 2004). Nevertheless, in 2014, Arsuaga et al. suggested that the SH sample should be removed from the *H. heidelbergensis* hypodigm due to the absence of derived Neanderthal features in the Mauer mandible, the holotype of this species. Moreover, in 2016 the nuclear DNA sequenced from two SH specimens indicated that these hominins belonged to the Neanderthal evolutionary lineage, being closely related to the ancestors of Neanderthals and sharing a common ancestor with Denisovans (Meyer et al., 2016). The state of preservation of the SH canines is generally good. There is a superficial loss of enamel on the

Table 1
Gran Dolina (GD) and Sima de los Huesos (SH) upper and lower permanent canines included in this study.
Tableau 1
Canines permanentes supérieures et inférieures de Gran Dolina (GD) et Sima de los Huesos (SH) incluses dans cette étude.

Specimen	Site	Individual	Tooth type	Root conservation	Wear stage
ATD6-1	GD	H1	33	Complete	2
ATD6-69	GD	H3	13	Incomplete	1
ATD6-13	GD	H1	23	Complete	2
AT-2759	SH	V	13	Complete	6
AT-144	SH	VII	13	Complete	6
AT-219	SH	XXVIII	13	Complete	6
AT-2388	SH	XXIV	13	Complete	2
AT-3192	SH	–	13	Complete	7
AT-3255	SH	XXVII	13	Complete	4
AT-5616	SH	–	13	Complete	5
AT-4335	SH	XII	13	Complete	3
AT-1942	SH	–	23	Incomplete	3
AT-2151	SH	XVIII	23	Incomplete	2
AT-44	SH	–	23	Complete	2
AT-5622	SH	–	23	Complete	3
AT-5621	SH	II	23	Complete	3
AT-6	SH	–	23	Complete	3
AT-1757	SH	–	23	Complete	3
AT-958	SH	–	23	Complete	5
AT-164	SH	–	33	Complete	3
AT-161	SH	–	33	Complete	4
AT-1755	SH	XV	33	Complete	5
AT-2762	SH	XXVIII	33	Complete	5
AT-567	SH	–	33	Complete	3
AT-578	SH	II	33	Complete	3
AT-67	SH	III	33	Incomplete	3
AT-6729	SH	XXIV	33	Incomplete	3
AT-2783	SH	XX	43	Incomplete	2
AT-1960	SH	XVI	43	Complete	3
AT-1951	SH	X	43	Complete	3
AT-2165	SH	XVIII	43	Incomplete	1
AT-3886	SH	XXV	43	Complete	2
AT-591	SH	VII	43	Complete	6
AT-593	SH	XXIII	43	Complete	3
AT-60	SH	I	43	Incomplete	3

Tooth type has been named following the World Dental Federation (FDI) system. Wear stages following Molnar (1971).
Le type de dent a été nommé suivant le système de la World Dental Federation (FDI). Stades d'usure selon Molnar (1971).

labial aspect of AT-578, and at the incisal mesial border of AT-145 the enamel is slightly chipped. The apical portion of the roots of AT-60, AT-67, AT-2783, AT-1942, AT-2151, AT-2165, AT-6729 and AT-808 are missing. There is one additional specimen from this site, AT-1144, that has not been included in this analysis because its root and crown are pathologically altered.

The TD6 and SH permanent canines from Atapuerca were compared with those belonging to the more recent (120–130 kyr) Neanderthal population sample of Krapina, Croatia (Brace, 1979; Martínez and Arsuaga, 1997; Rink et al., 1995; Wolpoff, 1979) (Appendix 1, see Table A.1). As a whole, the Krapina dental sample comprises 282 teeth, either isolated or preserved in jaws (Wolpoff, 1979). For the purposes of the present study, we used 18 canines (12 upper and six lower), generally in good preservation conditions; in this assemblage, only eight specimens have their roots complete.

In the analysis we also included a recent modern human (RMH) sample comprising a whole of 125 European and African specimens (Appendix 1, see Table A.2). This material comes from the anthropological collection housed at the Escuela de Medicina Legal of Madrid (Spain), the South African modern human bone collection permanently stored at the University of Pretoria (L'Abbé et al., 2005), and from Sudanese dental extractions (Elamin and Liversidge, 2013). In total, the modern human sample consists of 58 upper and 67 lower permanent canines from 81 individuals of both sexes.

In some cases, multiple teeth from the same individual were measured in the comparative samples, although only one antimere per individual was taken into consideration. We discarded teeth with any pathological damage affecting the mineralized tissues. Tooth crown wear stage was scored following Molnar (1971). Slightly worn teeth are those with a wear stage equal or below 3, characterized by the absence of the apex in the incisal border and the emergence of a point of dentine. In order to assess the effects of occlusal wear on such kind of studies dealing with tooth tissue proportions, we also compared those teeth with a wear degree of 4 (crown with minimal dentine patch), of 5 (crown with more extensive dentine patch), and of 6 (crown in which a lateral enamel loss is observed in the wear surface).

2.1. Micro-CT image acquisition and image processing

The isolated fossil teeth from Atapuerca were scanned using the Scanco Medical AG Micro-Computed Tomography 80 housed at the 'Centro Nacional de Investigación sobre la Evolución Humana' (CENIEH) in Burgos. Scans were performed employing two 0.1 mm copper filters and using a voltage of 70 kV and an amperage of 114 μA. The resultant slice thickness ranged between 18 and 36 micrometres (μm). Teeth included in mandibular and/or maxillary fragments were scanned using a Phoenix v/tome/x s (GE Measurement & Control) available in the same research centre. In this case, scans were performed by two 0.1 mm Copper filters, 100–120 kV voltage and 110–140 μA amperage, resulting isometric voxel ranging between 27 and 36 μm. Micro-CT data for the Krapina specimens (voxel size: 20–40 μm) were obtained from NESPOS© microtomographic database.

The majority of the teeth forming the recent modern human sample were scanned using the Phoenix microtomographic system housed at the CENIEH and the CTP-Mlab micro-CT equipment set at the Multidisciplinary Laboratory of the International Centre for Theoretical Physics (ICTP) of Trieste, Italy (Tuniz et al., 2013). All scans were performed by two 0.1 mm copper filters, 100–120 kV voltage and 110–140 μA amperage. The output images have a voxels size ranging between 17 and 21 μm. The South African specimens were scanned at the South African Nuclear Energy Corporation (Necsa), Pelindaba, using a Nikon XTH 225 ST equipment according to the following parameters: 100 kV voltage and 100 μA amperage. The final volumes were reconstructed with an isotropic voxel size ranging between 40.8 and 50.8 μm.

Image processing was performed using the Amira 6.0.0 software (Visage Imaging, Inc.). Dental tissues (enamel, dentine-pulp complex) were semi-automatically segmented using the Watershed Segmentation Tool and through manual editing. A non-local means filter was also applied. Small fractures and cracks were virtually filled in. We considered the cervical line as the fundamental morphological feature to isolate the crown and root (Benazzi et al., 2014). After anatomically orienting each tooth, we drew a straight line between the enamel maximum cervical extensions in the mesio-distal plane in all of the stacks of images. Finally, we made some corrections in the buccolingual planes. Accordingly, only the dentine contained in the enamel cap was classed as coronal dentine, which was limited to the base by a curve with a smooth surface and isolated from the root (for technical details, see García-Campos et al., 2018).

2.2. Measuring dental tissue components in 3D

On the virtually isolated crowns, the following variables were quantified following Olejniczak et al. (2008a): volume of the enamel cap (V_e, in mm^3); volume of the coronal dentine including the coronal pulp (V_{cdp}, in mm^3); surface area of the enamel-dentine junction (S_{EDJ}, in mm^2). These values were subsequently used to compute the 3D average enamel thickness index ($3DAET = V_e/S_{EDJ}$, in mm); the 3D relative enamel thickness index $\left(3DRET = 3DAET/\sqrt[3]{V_{cdp}}\right) \times 100$, scale free), the coronal volume ($V_c = V_e + V_{cdp}$, in mm^3), and the percentage of coronal volume that is dentine and pulp ($V_{cdp}/V_c = V_{cdp}/V_c \times 100$). Following Skinner et al. (2008a, b), we also assessed the outer surface of the enamel cap (S_{OE}, in mm^2) used to compute the relative outer enamel complexity ratio (OES/EDJS, free scale). Finally, the volume of the root dentine including the pulp (V_r, in mm^3) was assessed.

2.3. Statistical analyses

Statistical analyses were performed using the SPSS software (v. 18.0, SPSS Science, Inc.). Several statistical tests were employed to examine inter-taxon differences in tissue measurements, between the upper and lower canines, and by wear stages. In order to compare the crown variables, only slightly worn teeth (wear stages 1–3) were considered. Likewise, only the teeth bearing a complete root were used for root volume comparisons. Statistical tests were only applied when groups were represented by samples consisting of at least three cases. The normal distribution was assessed using the Shapiro–Wilk Test (when sample size was smaller than 50) and the Kolmogorov–Smirnov one-sample test with Lilliefors correction (when sample size was greater than 50). When normality could be assumed, we applied a Student's *t*-test; otherwise, we used the non-parametric Mann–Whitney *U*-test. Means were determined to be significantly different at the $\alpha = 0.05$ level.

2.4. Inter- and intra-observer errors

In order to estimate the intra- and inter-observer error, a sub-sample of seven teeth was analysed by two researchers (C.G.C. and M.M.M.). Each tooth was measured three times by both observers, who independently orientated, segmented, and isolated each specimen, and assessed each variable and index following the methods described above. The degree of error was estimated by calculating the inter- and intra-observer mean differences for each crown component measurement. The average intra-observer error was 1.59% (0.69–2.48%), whereas the average inter-observer error was 2.43% (1.72–3.15%). All values are within the accepted range.

3. Results

For each population examined in this study, the results of the 3D tooth tissue measurements (both absolute values and associated indices) are shown in Tables 2 and 3 and in Figs. 1 to 4. The results of the statistical analyses are provided in Tables 4 and 5.

3.1. Canine size variation

The canines of Krapina display the largest crown volume (V_c) values, whereas those of recent modern humans exhibit the lowest ones (Tables 2 and 3). Among the remainder groups, a marked reduction in V_c is noticeable in SH,

Table 2
Descriptive statistics for the measurements and indices associated with the slightly worn (1–3 wear stage following Molnar, 1971) upper canines in the study sample.
Tableau 2
Statistiques descriptives des mesures et des indices associés avec les canines supérieures légèrement usées (stades d'usure 1–3 d'après Molnar, 1971).

Taxonomic assignation	Population/Site		V_c	V_r	V_e	V_{cdp}	S_{EDJ}	S_{OE}	T_{3DAE}	T_{3DRE}	V_{cdp}/V_c	S_{OE}/S_{EDJ}
H. antecessor	Gran Dolina	N	2	1	2	2	2	2	2	2	2	2
		Mean	363.33	848.95	154.65	208.69	178.09	251.39	0.89	15.01	57.35	1.43
		SD	11.09	–	15.15	26.24	25.94	10.48	0.22	4.24	5.47	0.15
		SW	–	–		–	–	–	–	–	–	–
H. sp.	Sima de los Huesos	N	9	14	9	9	9	9	9	9	9	9
		Mean	327.28	679.83	146.12	180.75	166.39	226.64	0.88	15.68	55.10	1.36
		SD	35.34	119.73	14.25	23.62	16.41	17.52	0.05	1.19	2.08	0.08
		SW	0.76	0.03*	0.63	0.25	0.33	0.77	0.91	0.36	0.08	0.00*
H. neanderthalensis	Krapina	N	6	6	6	6	6	6	6	6	6	6
		Mean	403.59	800.28	169.93	233.66	188.56	260.91	0.9	14.65	57.83	1.39
		SD	60.63	132.06	23.23	37.94	20.27	26.23	0.04	0.69	1.16	0.03
		SW	0.01*	0.55	0.03*	0.00*	0.00*	0.00*	0.22	0.26	0.08	0.12
H. sapiens	Recent modern human sample of present study	N	56	58	56	56	56	56	56	56	56	56
		Mean	256.52	363.59	119.72	136.81	129.33	189.90	0.92	18.10	53.31	1.47
		SD	57.21	92.46	29.93	32.05	20.24	28.94	0.15	3.15	4.66	0.08
		SW	0.12	0.1	0.11	0.11	0.11	0.13	0.15	0.08	0.08	0.13

SD: standard deviation. SW: Shapiro Wilks test of normality (p-value). KS: *Kolmogorov*–Smirnov test of normality significance (p-value). Distributions were tested to be normal at the $\alpha = 0.05$ level (*).
SD : écart-type. SW : Test de normalité de Shapiro Wilks (p-value). KS : test de Kolmogorov–Smirnov de signification de la normalité (p-value). Il a été déterminé que les distributions sont normales au niveau $\alpha = 0{,}05$ (*).

Table 3
Descriptive statistics for the measurements and indices associated with the slightly worn (1–3 wear stage following Molnar, 1971) lower canines in the study sample.
Tableau 3
Statistiques descriptives des mesures et des indices associés des canines inférieures légèrement usées (stades d'usure 1–3 d'après Molnar, 1971).

Taxonomic assignation	Population/Site	V_c	V_r	V_e	V_{cdp}	S_{EDJ}	S_{OE}	T_{3DAE}	T_{3DRE}	V_{cdp}/V_c	S_{OE}/S_{EDJ}	
H. antecessor	Gran Dolina	*N*	1	1	1	1	1	1	1	1	1	1
		Mean	299.02	746.51	115.54	183.48	162.83	220.86	0.71	12.49	61.36	1.36
		SD	–	–	–	–	–	–	–	–	–	–
		SW	–	–	–	–	–	–	–	–	–	–
H. sp.	Sima de los Huesos	*N*	12	11	12	12	12	12	12	12	12	12
		Mean	244.57	537.47	107.15	137.42	140.46	189.91	0.76	14.88	56.11	1.35
		SD	34.35	143.94	14.48	21.85	16.91	21.69	0.06	1.5	2.4	0.03
		SW	0.87	0.03*	0.54	0.17	0.14	0.56	0.57	0.6	0.36	0.85
H. neanderthalensis	Krapina	*N*	4	2	4	4	4	4	4	4	4	4
		Mean	353.43	794.35	139.77	213.66	179.38	242.92	0.78	13.06	60.38	1.36
		SD	58.21	26.86	21.35	37.72	22.16	26.35	0.04	0.65	1.39	0.04
		SW	0.34		0.58	0.66	0.42	0.64	0.89	0.13	0.38	0.98
H. sapiens	Recent modern human sample of present study	*N*	54	67	54	54	54	54	54	54	54	54
		Mean	209.25	327.11	95.83	113.41	119.62	171.43	0.8	16.72	54.17	1.44
		SD	40.89	79.74	21.02	24.41	16.64	22.58	0.14	3.03	4.69	0.082
		KS	0.08	0.08	0.1	0.07	0.11	0.06	0.08	0.08	0.08	0.11

SD: standard deviation. SW: Shapiro–Wilks test of normality (p-value). KS: *Kolmogorov*–Smirnov test of normality significance (p-value). Distributions were tested to be normal at the $\alpha = 0.05$ level (*).
SD : écart-type. SW : Test de normalité de Shapiro–Wilks (p-value). KS : test de Kolmogorov–Smirnov de la signification de la normalité (p-value). Il a été déterminé que les distributions sont normales au niveau $\alpha = 0{,}05$ (*).

whose values clearly overlap the extant human range of variation. In fact, the differences between SH and RMH for the upper canines are not significant (p-value = 0.357), while for the lower canines SH shows significantly larger crown dimensions (p-value = 0.006) (Table 4). The V_c values of the canines of the early Pleistocene sample of Gran Dolina TD6 fall mid-way between the middle Pleistocene sample of Atapuerca-SH (with smaller crowns) and Krapina (with larger crowns), near Krapina's lower range.

For the root volume (V_r), a marked size reduction compared to the European early and middle Pleistocene groups is noticeable in recent humans (Tables 2 and 3). Both maxillary and mandibular canine roots are large in *H. antecessor* and overlap the SH and Krapina ranges. In spite of such similarity, SH root dimensions fall mid-way between the Neanderthal (larger values) and the recent modern human (lower values) estimates and are significantly different to both (p-values < 0.05), even if it is closer to the former

(Table 4). In some specific cases, the SH root volumes overtake the Krapina's variation range (spec. AT-591 and AT-145).

With the exception of the Neanderthal sample, in all groups examined in this study, the V_c values of the maxillary canines are significantly larger than those measured in the mandibular ones, and the same is true for the V_r (Table 5).

3.2. Dental tissue proportions

The marked canine size variation is also reflected in the absolute tissue dimensions (Table 4 and Figs. 1 and 2). Here again, the enamel volume (V_e) and the coronal dentine-pulp complex volume (V_{cdp}) values of RMH are smaller, partially due to the smaller of the canine crown size, whereas *H. neanderthalensis* have larger magnitudes of both dental tissues (Table 4). With the exception of the lower canine V_e, both variables (V_e and V_{cdp}) differ significantly between the SH and Krapina samples (p-values < 0.05), exhibiting the first population's lower values (Table 4). Conversely, in SH, the V_e values of the maxillary canine approach those of the extant human estimates. Once again, *H. antecessor*'s V_e and V_{cdp} values are intermediate between SH (lower volumes) and *H. neanderthalensis* (greater dimensions) in both tissues, but overlap with the variation range expressed by both samples (Figs. 1 and 2). The outer enamel surface (OES) and the enamel–dentine junction surface (EDJS) areas show distribution patterns comparable to those described for V_e and V_{cdp}, respectively (Table 4).

When the interpopulation differences are considered for each index (3DAET, 3DRET, V_{cdp}/V_c and OES/EDJS), we observe that, although RMH canines have absolutely smaller enamel cap volumes, their relative thickness (3DRET) is significantly greater than measured in the other samples (p-values < 0.05) (Table 4 and Figs. 1 and 2). Likewise, the fossil *Homo* samples have smaller OES/EDJS values than those measured in extant humans. Lastly, the canines from TD6, SH and Krapina display a higher percentage of crown volume that is a dentine-pulp complex (V_{cdp}/V_c), whereas this index is lower in the extant human sample (Figs. 1 and 2).

The differences in upper and lower canine dimensions are also reflected in their tissue components (V_e and V_{cdp}), being absolutely larger in the upper canines. The same is true for EDJS and OES. Contrary to the remainder, in the Neanderthal sample, the mean values of the absolute measurements assessed on the upper and lower canines are not significantly different, except for the values of V_e (Table 5). On the other hand, the average and relative enamel thickness (3DAET, 3DRET) is higher in the upper canines. SH is the only population in which the 3DRET is similar in both canines. Differently from the enamel, in all groups the V_{cdp}/V_c values are higher in the mandibular canines, even if the differences are not significant, except in the case of *H. neanderthalensis* (p-value = 0.011). The OES/EDJS values are similar in the upper and lower teeth of the SH and Krapina samples. However, this index is greater in the *H. antecessor* and modern human upper canines, but statistically different only in the latter group.

3.3. Enamel thickness distribution

The colour maps shown in Figs. 3 and 4 reflect patterns of enamel distribution, in which the thickest enamel is represented in red and the thinnest in blue. These maps support the 3DAET and 3DRET results noted. Overall, in both maxillary and mandibular canines of all population examined, the enamel cap is thicker on the buccal aspect, especially on the cuspal half of the crown; conversely in the cervical portion is relatively and absolutely thinner. However, whereas in the upper canines the thicker enamel is homogeneously spread out (involving both distal and mesial marginal ridges), in the lower ones the thickest values are more distally placed. In the *H. antecessor*, SH and Krapina mandibular canines, the enamel cap is thicker on the distal than on the mesial crown aspect, and is especially thick at the level of the distal marginal ridge. Among the fossil samples, Krapina shows the lowest thickness values. However, although the RMH lower canines also exhibit thicker enamel on the distal aspect, thickened enamel is found in the rest of the incisal half of the buccal surface, till the marginal ridge. Likewise, although the enamel thickness patterns of upper canines (Fig. 3) seem to be common in all groups, in RMH the greater thickness spreads to the half of the crown.

3.4. The impact of dental wear

The descriptive statistics of the indices obtained from the measures performed on the subset of more extensively worn teeth (degrees 4 to 6; Molnar, 1971) are shown in the Appendices, Tables B.1 and B.2. As expected from the enamel thickness distribution maps (Figs. 3 and 4), occlusal wear affects the dental tissue proportions and a greater variation is observed as wear increases. As it was predictable, in all samples the enamel thickness (3DAET, 3DRET) values are lower in the more extensively worn crowns. In general, the percentage of variation of the indices is greater in the upper canines. On the other hand, the V_{cdp}/V_c values are larger in more worn teeth, mainly due to enamel volume reduction. Each species represented in this study is affected by wear in a different way, so their indices neither increase nor decrease in the same way.

4. Discussion

At present, the phylogenetic meaning of dental enamel and dentine proportions is still unclear; furthermore, how it interacts with the different functional demands or developmental restrictions is not fully understood. However, the study of these traits could represent an important source of information, since dental tissue patterns have been linked to changes in dental size (Kupczik and Hublin, 2010; Lieberman, 2011), EDJ surface morphology (Smith et al., 2005), enamel secretions rates (Grine, 2005; Grine and Martin, 1988), dental formation time variation (Smith et al., 2005), or even to changes in physiological signals (Goldberg et al., 2011; Plavcan, 2012; Smith et al., 2012).

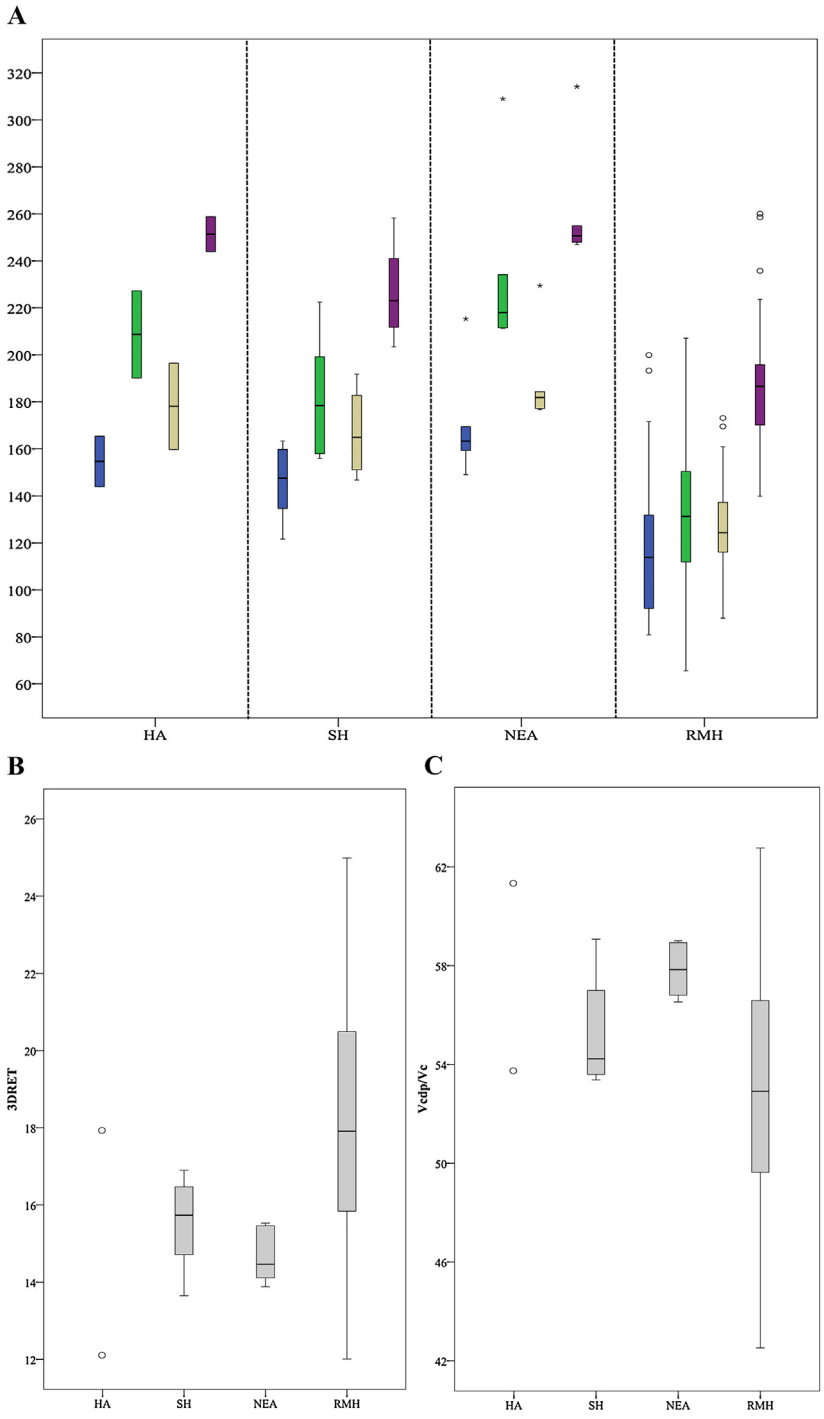

Fig. 1. Standard box and whisker plot of the upper canine tissue proportions (wear stages 1–3). Groups are arranged in chronological order: *Homo antecessor* (HA), Sima de los Huesos (SH), Krapina (NEA), and recent modern human (RMH). (A) Absolute enamel and dentine volume and surface dimensions: V_e (blue), V_{cdp} (green), EDJS (brown), OES (violet). (B) Relative enamel thickness (3DRET) comparison. (C) Percentage of coronal volume that is dentine and pulp (V_{cdp}/V_c) comparison. This graph represents the interquartile range (25^{th}–75^{th} percentiles: boxes), 1.5 interquartile ranges (whiskers) and the median values (black line). Outliers are signified with circles and asterisks.

Fig. 1. Diagrammes en boîte des proportions des tissus dentaires des canines supérieures (stades d'usure 1–3). Les groupes sont organisés par ordre chronologique : *Homo antecessor* (HA), Sima de los Huesos (SH), Krapina (NEA) et humains modernes récents (RMH). (A) Dimensions des volumes et surfaces absolus d'émail et de dentine : V_e (bleu), V_{cdp} (vert), S_{EDJ} (marron), S_{OE} (violet). (B) Comparaisons relatives de l'épaisseur de l'émail (T_{3DRE}). (C) Comparaisons du pourcentage du volume de la couronne, incluant dentine et pulpe (V_{cdp}/V_c). Ce graphique montre les écarts interquartiles (percentiles à 25–75 : boîtes), les écarts interquartiles à 1,5 (moustaches) et la valeur médiane (ligne noire). Les valeurs aberrantes sont indiquées par des cercles et astérisques.

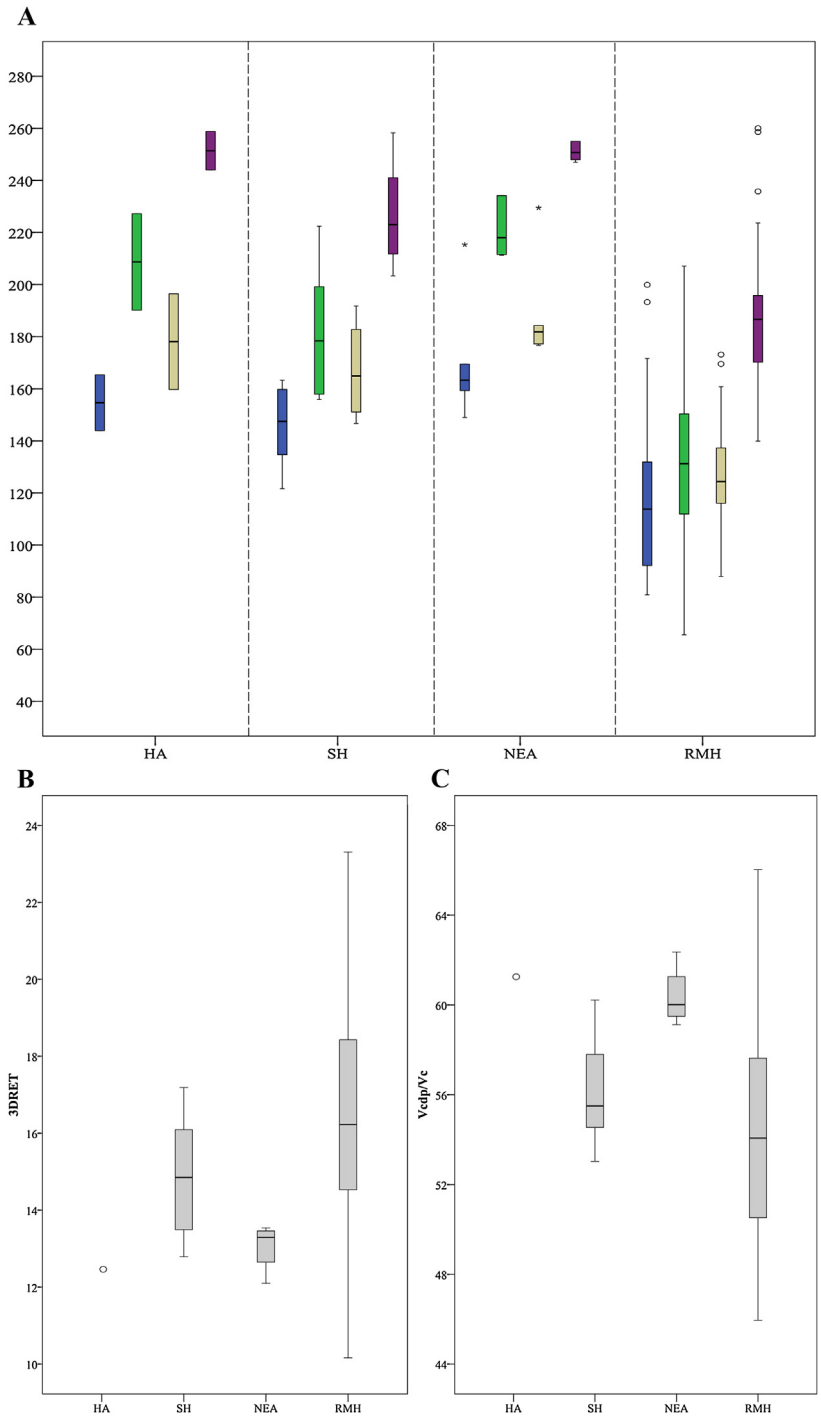

Fig. 2. Standard box and whisker plot of the lower canine tissue proportions. Groups are arranged in chronological order: *Homo antecessor* (HA), Sima de los Huesos (SH), Krapina (NEA), and recent modern human (RMH). (A) Absolute enamel and dentine volume and surface dimensions: V_e (blue), V_{cdp} (green), EDJS (brown), and OES (violet). (B) Relative enamel thickness (3DRET) comparison. (C) Percentage of coronal volume that is dentine and pulp (V_{cdp}/V_c) comparison. This graph represents the interquartile range (25^{th}–75^{th} percentiles: boxes), 1.5 interquartile ranges (whiskers), and the median values (black line). Outliers are signified with circles and asterisks.

Fig. 2. Diagrammes en boîte des proportions des tissus dentaires des canines inférieures (stades d'usure 1–3). Les groupes sont organisés par ordre chronologique : *Homo antecessor* (HA), Sima de los Huesos (SH), Krapina (NEA) et humains modernes récents (RMH). (A) dimensions des volumes et surfaces absolus d'émail et de dentine : V_e (bleu), V_{cdp} (vert), S_{EDJ} (marron), and S_{OE} (violet). (B) Comparaisons relatives de l'épaisseur de l'émail (T_{3DRE}). (C) Comparaisons du pourcentage de volume de la couronne, incluant dentine et pulpe (V_{cdp}/V_c). Ce graphique montre les écarts interquartiles (percentiles à 25–75 : boîtes), les écarts interquartiles à 1,5 (moustaches) et la valeur médiane (ligne noire). Les valeurs aberrantes sont indiquées par des cercles et des astérisques.

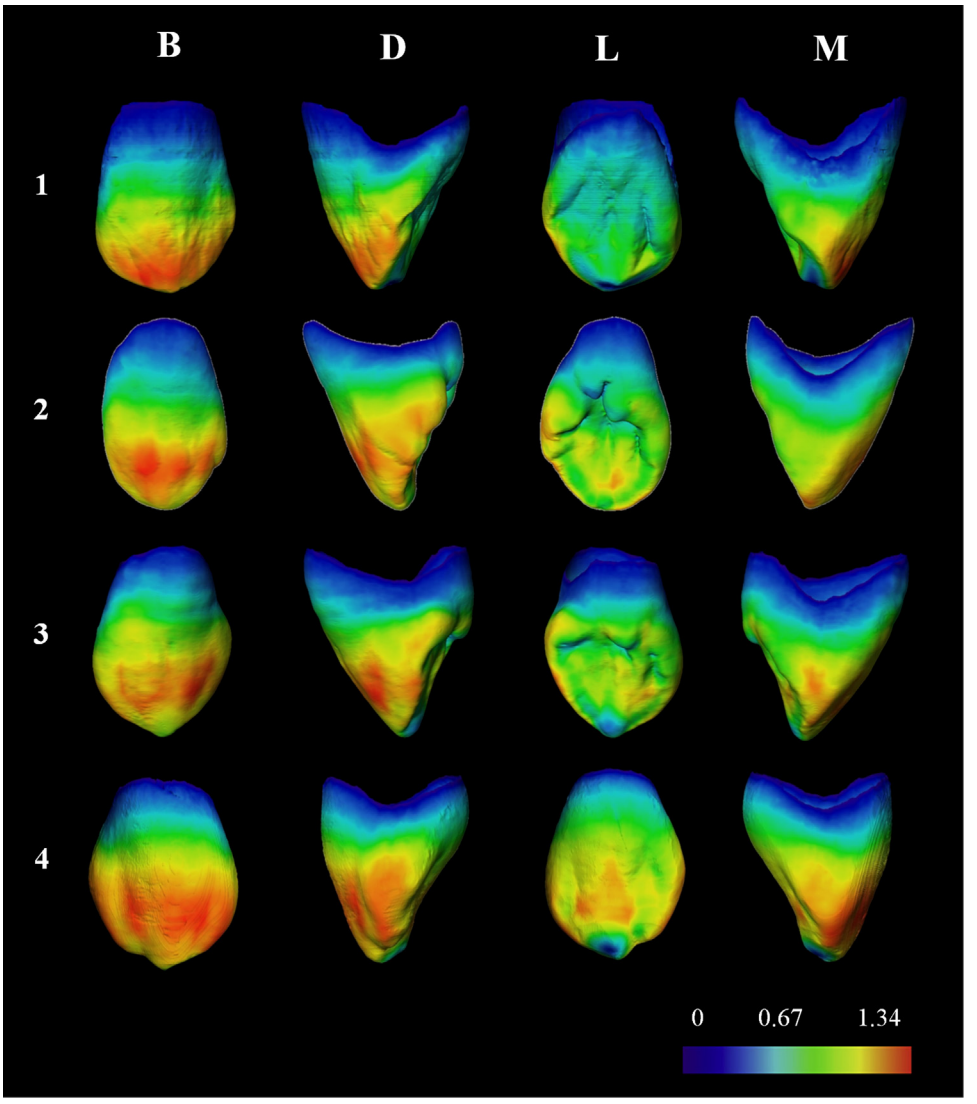

Fig. 3. 3D enamel thickness distribution maps of upper canines (wear stages 1–3). This figure represents the 3D maps obtained through the computing of the distance between two triangulated surfaces (EDJS and OES) in which, for each vertex of one surface, it is computed the closest point on the other surface. The results are visualized using spectral colours, where the largest distance (thickest enamel) is represented in red and the shortest (thinner enamel) enamel in blue. Colour scale: 0–1.34 mm. The subsample represented comprises: *H. antecessor*, ATD6-13 (1); Sima de los Huesos, AT-2151 (2); Krapina, D102 (3); recent modern human, UCM3 (4). All the teeth represented are left canines; right canines have been mirrored. Views: buccal (B), distal (D), lingual (L) and mesial (M).

Fig. 3. Cartographies 3D de distribution de l'épaisseur de l'émail des canines supérieures (stades d'usure 1–3). Cette figure représente les cartographies 3D obtenues par le calcul de la distance entre deux surfaces triangulées (S_{EDJ} et S_{OE}). La distance entre chacun des vertex les plus proches des deux surfaces est alors calculée. Les résultats sont visualisés en utilisant des couleurs spectrales, où la plus grande distance (l'émail le plus épais) est représentée en rouge et celle la plus courte (émail plus fin) en bleu. Échelle de couleur : 0–1,34 mm. Le sous-échantillon représenté comprend : *H. antecessor*, ATD6-13 (1) ; Sima de los Huesos, AT-2151 (2) ; Krapina, D102 (3) ; un humain moderne récent, UCM3 (4). Toutes les dents représentées sont des canines gauches ; les canines droites sont représentées par leur image miroir. Vues : buccale (B), distale (D), linguale (L) et mésiale (M).

By means of this comparative study, we have assessed the three-dimensional tissue proportions of the early and middle Pleistocene populations of Atapuerca, and we have compared them with those observed in Neanderthals and recent modern humans. Through this study, we intend to contribute to the knowledge of the evolutionary trends and taxonomically distinct patterns of early European hominin dental tissues, which is a crucial step for understanding the appearance of the typically Neanderthal derived traits during the middle Pleistocene.

4.1. Size variation and dental tissue proportions of Neanderthal canines

In contrast to the posterior dentition, latter *Homo* species anterior tooth crowns and roots have been

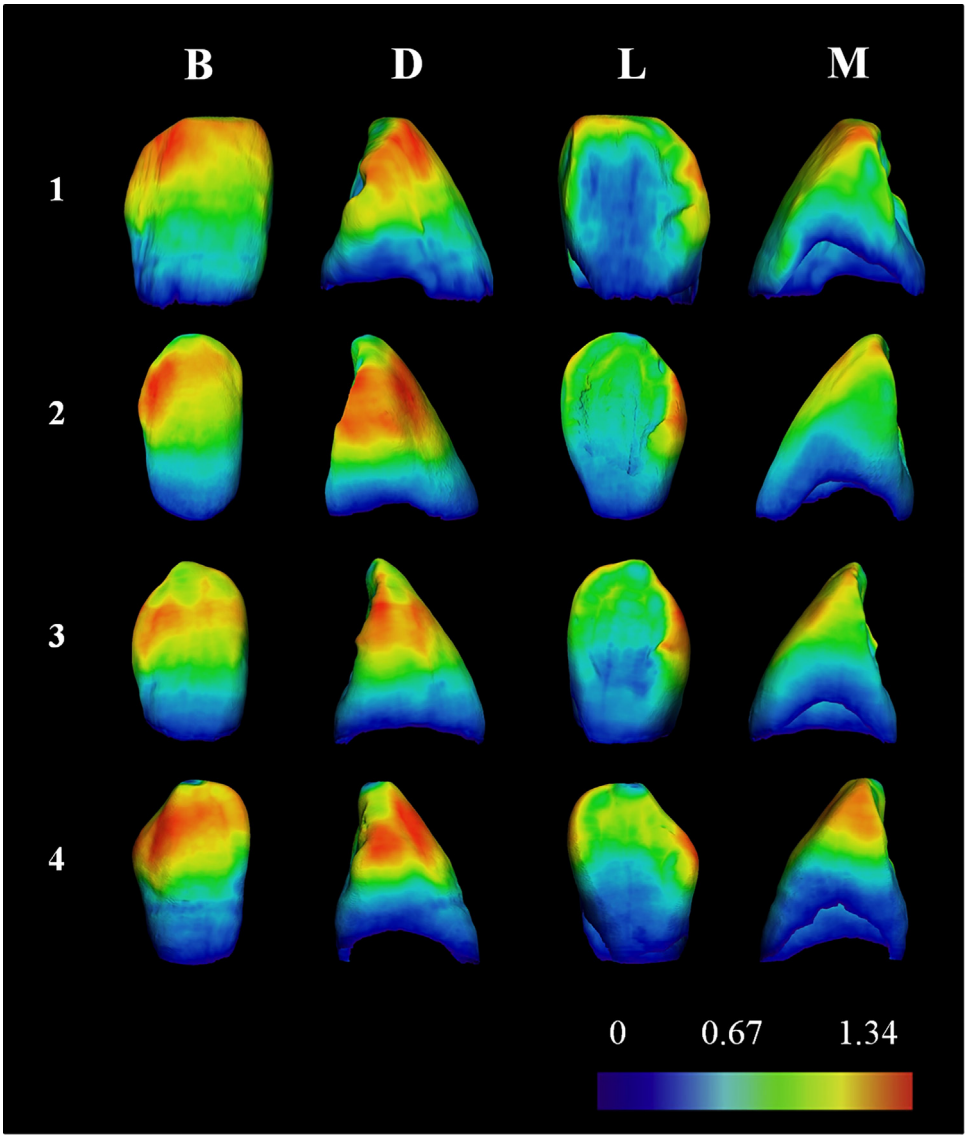

Fig. 4. 3D enamel thickness distribution maps of lower canines (wear stages 1–3). This figure represents the 3D maps obtained through the computing of the distance between two triangulated surfaces (EDJS and OES) in which, for each vertex of one surface, it is computed the closest point on the other surface. The results are visualized using spectral colours, where the largest distance (thickest enamel) is represented in red and the shortest (thinner enamel) enamel in blue. Colour scale: 0–1.34 mm. The subsample represented comprises: *H. antecessor*, ATD6-1 (**1**); Sima de los Huesos, AT-2783 (**2**); Krapina, D121 (**3**); recent modern human, UCM51 (**4**). All the teeth represented are right canines; left canines have been mirrored. Views: buccal (B), distal (D), lingual (L) and mesial (M).

Fig. 4. Cartographies 3D de distribution de l'épaisseur de l'émail des canines inférieures (stades d'usure 1–3). Cette figure représente les cartographies 3D obtenues par le calcul de la distance entre deux surfaces triangulées (S_{EDJ} et S_{OE}). La distance entre chaque vertex les plus proches des deux surfaces est alors calculée. Les résultats sont visualisés en utilisant des couleurs spectrales, où la plus grande distance (l'émail le plus épais) est représentée en rouge, et celle la plus courte (émail plus fin) en bleu. Échelle de couleur : 0–1,34 mm. Le sous-échantillon représenté comprend : *H. antecessor*, ATD6-13 (1) ; Sima de los Huesos, AT-2151 (2) ; Krapina, D102 (3) ; un humain moderne récent, UCM3 (4). Toutes les dents représentées sont des canines droites ; les canines gauches sont représentées par leur image miroir. Vues : buccale (B), distale (D), linguale (L) et mésiale (M).

described as increasing in size in comparison with previous hominin taxa, being this increment more pronounced in Neanderthals, who even exceed the dimensions of *H. sapiens* (Buti et al., 2017; Wolpoff, 1999). The Neanderthal incisors are known to be especially large relative to the rest of dentition (Wolpoff, 1979). Our results show that Neanderthal canine crowns were also larger than those of *H. sapiens*, which agrees with Buti et al. (2017). This increase in size is especially pronounced in the lower canines, which reach similar dimensions to those of the upper canines, a characteristic which is not observed in any other among the species included in this study (Table 5). Neanderthal

Table 4
Inter-specific mean comparison analysis (*p*-value) of the dental tissue components between the slightly worn canines of Sima de los Huesos (SH), Krapina (NEA), and recent modern humans (RMH).
Tableau 4
Analyse interspécifique de comparaison des moyennes (*p*-value) des composants des tissus dentaires entre les canines supérieures et inférieures légèrement usées de Sima de los Huesos (SH), Krapina (HN) et humains modernes récents (RMH). Le *t*-test de Student a été employé lorsque les variables étaient normalement distribuées.

	Comparison	V_c	V_r	V_e	V_{cdp}	*EDJS*	*OES*	*3DAET*	*3DRET*	V_{cdp}/V_c	OES/EDJS
Upper canines	SH/NEA	**0.000***	**0.021***	**0.000***	**0.000***	**0.001***	**0.000***	**0.002***	**0.689**	**0.936**	**0.153**
	SH/RMH	0.357	**0.000***	0.165	0.006*	0.009*	0.641	0.000*	0.000*	0.000*	**0.000***
	NEA/RMH	**0.000***	**0.000***	**0.002***	**0.000***	**0.000***	**0.000***	**0.001***	**0.000***	**0.000***	**0.000***
Lower canines	SH/NEA	0.006*	–	0.054	0.003*	0.007*	0.005*	0.669	0.055	0.441	0.752
	SH/RMH	0.000*	**0.000***	0.023*	0.000*	0.000*	0.005*	0.154	0.000*	**0.000***	**0.000***
	NEA/RMH	0.000*	–	0.000*	0.000*	0.000*	0.000*	0.710	0.000*	0.000*	0.000*

The Student *t*-test was employed when the variables were normally distributed. In the remaining cases, the Mann–Whitney *U* test was applied (in bold). Means were determined to be significantly different at the $\alpha = 0.05$ level (*).
Dans les autres cas, le test *U* de Mann–Whitney (en gras) a été appliqué. Il a été déterminé que les moyennes étaient significativement différentes au niveau $\alpha = 0{,}05$ (*).

Table 5
Intra-specific mean comparison analysis (*p*-value) of the dental tissue components and between lower and upper slightly worn canines of Sima de los Huesos (SH), Krapina (NEA), and recent modern humans (RMH).
Tableau 5
Analyse intraspécifique de comparaison des moyennes (*p*-value) des composants des tissus dentaires entre les canines supérieures et inférieures de Sima de los Huesos (SH), de Krapina (HN) et des humains modernes récents (RMH). Le *t*-test de Student a été employé lorsque les variables étaient normalement distribuées.

	V_c	V_r	V_e	V_{cdp}	*EDJS*	*OES*	*3DAET*	*3DRET*	V_{cdp}/V_c	*OES*/EDJS
SH	0.000*	**0.011***	0.000*	0.001*	0.003*	0.001*	0.000*	0.302	**0.355**	**0.094**
NEA	**0.670**	0.954	**0.033***	**0.670**	**0.670**	**0.670**	0.002*	0.006*	**0.011***	0.236
RMH	0.000*	0.034*	0.000*	0.000*	0.054	0.002*	0.000*	**0.014***	**0.452**	0.009*

The Student *t*-test was employed when the variables were normally distributed. In the remaining cases, the Mann–Whitney U test was applied (in bold). Means were determined to be significantly different at the $\alpha = 0.05$ level (*).
Dans les autres cas, le test *U* de Mann–Whitney (en gras) a été appliqué. Il a été déterminé que les moyennes étaient significativement différentes au niveau $\alpha = 0{,}05$ (*).

and recent modern human anterior teeth also differ for their root size. Le Cabec et al. (2013) observed that Neanderthals have larger anterior roots dimensions than recent modern humans, which is supported by our results. These authors also noted that the anterior roots of the early and middle Pleistocene specimens were at least as large as in Neanderthals, thus concluding that Neanderthal root dimensions could result from the retention of an ancestral condition.

Despite the shortage of comparative data of anterior teeth tissue proportions currently limits the possibility of assessing evolutionary patterns in a reliable way, the available evidence suggests that the changes in canine crown size of Neanderthals can be preferentially attributed to shifts in the volume of the dentine–pulp complex, whereas enamel volume represents a minor role (Buti et al., 2017). Our results support this statement. Although it has been observed that *H. neanderthalensis* canines have a significantly larger enamel volume (V_e) than *H. sapiens*, the increment in their dentine-pulp complex (V_{cdp}, V_{cdp}/V_c) is even greater, which, together with larger and more complex EDJ surfaces (EDJS, OES/EDJS), results into relatively lower enamel thickness (3DRET) values. Such differences are also expressed in the patterns of enamel distribution showed in Figs. 3 and 4. The tooth canine assemblage from Krapina shows lower enamel thickness values than measured in our recent modern human sample, which is reflected in a less intense red colour. It also can be observed that in modern humans the areas with greater enamel thickness values are more widely spread through the buccal surface of the crown, especially in lower canines.

Therefore, these results support the first hypothesis and show that, together with a number of characteristic morphological features (Gómez-Robles, 2010; Gómez-Robles et al., 2012; Kupczik and Hublin, 2010; Martinón-Torres et al., 2012, 2014; Martínez de Pinillos et al., 2014), crown and root size, as well as dental tissue proportions, represent useful indicators to discriminate between the Neanderthal and *H. sapiens* lineages.

In an evolutionary perspective, a point of major interest concerns the assessment of the time when such tooth structural differences between the two lineages emerged. With this respect, Buti et al. (2017) assessed dental tissue proportions of early modern human (EMH), Upper Palaeolithic modern human (UPMH) and recent modern human (RMH) canine teeth and separately compared them with those of Neanderthals. In contrast to later *H. sapiens* populations, they observed that EMH canines are within the range of variation of Neanderthals for all crown tissue components (V_e, V_{cdp}, EDJS). Similar results were obtained by Smith et al. (2012) in a study on 2D dental tissue measurements variation within the genus *Homo*, where it has been concluded that differences across the dentition are less

pronounced between Neanderthals and fossil *H. sapiens* than between Neanderthals and recent *H. sapiens*. The same conclusion was reached by Le Cabec et al. (2013) about root dimensions. As a whole, these results provide evidence that the anterior teeth tissue proportions and root size typical of extant populations appeared late in time. Specifically, this suggests that enamel thickness in modern humans may not be the result of a plesiomorphic trait retention. However, whereas it has been suggested that large root can be considered a primitive condition (Le Cabec et al., 2012, 2013), the question of when the overall thinly enameled pattern emerged in the Neanderthal lineage is still unresolved.

4.2. Similarities and differences in dental tissue patterns of Atapuerca samples and H. neanderthalensis canine teeth

The dentition of the middle Pleistocene population of Sima de los Huesos presents most of the morphological traits usually considered characteristic of the Neanderthals (Martinón-Torres et al., 2012), displaying an expression of 'mass additive' features in their anterior dentition (Irish, 1998; Martinón-Torres et al., 2012). The derived conformation of SH teeth contrasts with that of other penecontemporaneous populations such as that of Arago (Bermúdez de Castro et al., 2018), even overtaking some classic Neanderthals like those of Krapina, Hortus and Le Moustier (Gómez-Robles, 2010; Gómez-Robles et al., 2007, 2008, 2011). Regarding the tooth size variation, the metric features of the Atapuerca–SH dental remains correspond to the evolutionary pattern characterizing the middle Pleistocene populations. Although SH canine and incisor sizes are large in relation with molar size, showing an expansion in their anterior teeth, their dentition is characterized by their small dimensions (Bermúdez de Castro, 1986). The results from this study reassert the reduced crown volume of their canines in comparison to those of Neanderthals, reaching a similar size to that of modern humans. This reduction is less marked in their roots, which, despite having volumes statistically smaller than those of Neanderthals, clearly falls into their range of variation, showing, perhaps, its more conservative nature. However, in spite of their size, SH canine crowns comprise similar percentages of dentine (upper canines: $55.10 \pm 2.08\%$; lower canines: $56.11 \pm 2.40\%$) than those of Neanderthal populations (upper canines: $57.83 \pm 1.16\%$; lower canines: $60.38 \pm 1.39\%$), as well as similar EDJ surface complexity (OES/EDJS values). As a result, the 3DRET of their upper and lower canines falls into the variation range of *H. neanderthalensis*, being statistically similar. Likewise, the enamel thickness coloured maps (Figs. 3 and 4) show that SH and Krapina populations share the general pattern of enamel thickness distribution, both in the upper and lower canines.

On the other hand, *H. antecessor* is defined by a unique mosaic of: primitive traits, shared with early *Homo* species, and derived features, some of them present in modern humans and others shared with Neanderthals and SH (Bermúdez de Castro et al., 1999a, 2015; Martinón-Torres et al., 2012). Despite the fact that most of the dental traits of the Atapuerca early Pleistocene homonins are primitive, which align them with *H. ergaster*, *H. erectus* and some African early and middle Pleistocene specimens (Bermúdez de Castro et al., 2015), the permanent lower and upper canines of *H. antecessor* are morphologically derived with regard to the *Homo* clade (Martinón-Torres et al., 2008). Moreover, *H. antecessor* shares with European middle Pleistocene groups the expansion of the anterior teeth, particularly in the upper canines, which are near to the maximum range recorded for the genus *Homo* (Bermúdez de Castro et al., 1999a). Our results corroborate the large canine crown and root volumes of Gran Dolina population, being encompassed into the range of Neanderthals (near the minimum in the case of the crowns) but greater than SH teeth. Their absolute dental tissue measurement values (V_e, V_{cdp}, EDJS and OES) are also intermediate between those of *H. neanderthalensis* and SH hominins, but similar to both (Figs. 1 and 2). As a result, *H. antecessor* shares with these species the dental tissue proportions of its permanent canines (Tables 2 and 3). Likewise, their pattern of enamel thickness distribution shown in the colour maps (Figs. 3 and 4) is closer to that of *H. neanderthalensis*, although not as much to that of SH.

Canine dental tissue proportions results showed above support the second hypothesis. The noticeable similarities between SH and Krapina dental tissue proportions indicate that thinly enamelled pattern cannot be considered as an autapomorphic Neanderthal trait but a homologous trait shared with at least the middle Pleistocene hominins from Atapuerca. On the contrary, our results appear to reject the third hypothesis, since Gran Dolina canines seem to exhibit thinly enamelled pattern, a feature that is shared with SH hominins and Neanderthals anterior dentition. This would moves backwards the timing for the appearance of the thinner enamel derived feature to around 800 kyr ago, suggesting that the relatively thin enamel might be a primitive trait in Neanderthals. However, the scarce *H. antecessor* sample size forces us to take these results with caution, and wait for new studies on the rest of their dentition to be published. On the other hand, these results seem to support the existence to certain similarity between the Atapuerca populations and the African *H. erectus/ergaster*, distinguishing them from the thickly-enamelled Asiatic *H. erectus* (Smith et al., 2012; Zanolli, 2014). Once again, future studies about posterior dentition tissue patterns will be those which solve this issue.

Lastly, the large size of the canine roots of both *H. antecessor* and SH population supports the primitive polarity of this trait, highlighting that big root dimensions seems to be associated in some way with the large dentine-pulp complex percentages in their crowns.

4.3. The influence of the dental wear on taxonomic studies on dental tissue proportions

Our study shows that wear affects the taxonomical comparison of enamel and dentine dimensions (in agreement with Buti et al., 2017), supporting the last

hypothesis proposed in this study. The enamel thickness coloured maps show that in all species examined enamel is thicker in the incisal area of the buccal view. Therefore, the more pronounced the wear is, the less noticeable are the inter-specific differences. Additionally, the patterns of enamel thickness distribution change within species so they are affected in a different manner by this erosive process, making it difficult compare them. So although in many cases there is no other option than to compare teeth with similar stages of wear, due to the lack of slightly worn teeth samples, the conclusions obtained from this comparison should be taken with caution.

4.4. Broader implications of the dental tissue proportion variation

Many hypotheses have been proposed to explain the adaptive significance of dental tissue variation. Some authors have interpreted the variation of molar enamel and dentine amounts as a response to changes in functional demands, associated with the increase of the resistance as a result of the consumption of more abrasive foods (Lucas et al., 2008). However, there do not appear to be clear differences in the relative enamel thickness thresholds between hard- and soft-object feeders, which suggests that dietary inferences based on enamel thickness are not necessarily accurate (Dumont, 1995; Smith et al., 2012). Moreover, these inferences may be complicated by non-masticatory behaviours (Constantino et al., 2011; Hall and Schaller, 1964; Martin et al., 2003). On the other hand, the attrition of the thinly enamelled Neanderthal anterior teeth has been often compared with that of current groups such as the Inuit and Australian Aborigines (Hinton, 1981; Molnar, 1971), who show the highest rates of attrition within modern human populations. Other authors have proposed that the amount of enamel is the result of both the enamel secretion rates and the formation times of teeth (Grine and Martin, 1988). Nevertheless, once again, Neanderthal molars, as well as canines, seem to have secretion rates and crown formation times that do not significantly differ from those of modern human (Dean, 2009; Dean et al., 2001). However, these authors might on the right track since a combination of similar secretion rates and formation times with larger EDJ surfaces areas might be behind the decrease in enamel thickness in Neanderthal teeth. In this framework, relative enamel thickness variation may be, therefore, interpreted primarily as a consequence of changes in the coronal amount of dentine more than in the enamel cap.

Following this reasoning, it is important to notice that the degree of variation of molars dentine usually appears correlated with changes in root dimensions and craniofacial morphology (Kupczik and Hublin, 2010; Lieberman, 2011). Likewise, some studies have linked the large anterior dentition of Neanderthals with the increase of their craniofacial skeleton (Anton, 1990; Hublin, 1998; Trinkaus, 1987). This association may suggest similarities in dentine and bone tissue response to different physiological changes, possibly as a result of a common ontogenetic development and similar organic composition, which differentiates them from the enamel component (Plavcan, 2012; Smith et al., 2012). The Growth Hormone (GH)/Insulin-like growth factor I (IGF-I) axis might to be behind both tissues regulation. This hormonal axis is a major regulator of postnatal growth and development (Giustina and Veldhuis, 1998), which has a strong influence on the metabolism of bone and oral tissues (Slootweg, 1993). GH directly acts on the osteoblast to stimulate bone formation (Nishiyama et al., 1996). Likewise, this hormone is able to induce the proliferation of epithelial steam cells and Hertwig's epithelial root sheath, the preodontoblast differentiation and the dentine matrix formation (Young et al., 1992).

According to the GH/IGF-I axis influence hypothesis, the increase in the amount of dentine should appear associated with larger cranial and postcranial robustness. SH specimens share derived facial, dental, mandibular, and glenoid features with Neanderthals, which overall lead to a functional masticatory complex similar in both groups, more robust to those from modern humans (Arsuaga et al., 2014; Harvati et al., 2011). On the other hand, in a study by Arsuaga et al. in 2015, in which SH postcranial morphology was compared to that of other *Homo* species, the authors concluded that SH may be included in 'wide *Homo*' bauplan, showing wide and heavy bodies whose parameters (stature and body mass) were largely maintained in European middle Pleistocene groups, including Neanderthals (Arsuaga et al., 2015). Estimates of body proportions in *H. antecessor* suggest that TD6 males presented similar stature and body mass to Sima de los Huesos male individuals (Pablos et al., 2012, 2017), reflecting a marked robustness, which contrasts with their face gracility (Bermúdez de Castro et al., 2008; Rosas and Bermúdez de Castro, 1999). Therefore, although it could be very risky to try to directly relate changes in the dentine-pulp complex with shifts in bone robustness, all these evidences seem to show the existence of parallel responses in dentine and bone tissues in the face of identical physiological signals.

5. Conclusions

In conclusion, our results on the tissue proportions of early and middle Pleistocene populations of Atapuerca seem to indicate an early enamel thickness decrease in permanent canines. The thinly enamelled pattern seems to be already observed 0.80–0.88 Ma ago in *H. antecessor*, as well as in later populations such as Sima de los Huesos and Neanderthal individuals, maybe as a result of the relatively dentine-pulp complex expansion and the increase in the complexity of the EDJ surface of these populations. A greater role of the coronal dentine component seems to be accompanied by larger roots, and might be related with more bone robustness. Future studies of tissue proportion of anterior dentition of early *Homo* species could help to increase the comparative sample and to gain a better understanding of dental histological trends and polarity. Particularly, it would be interesting to explore the dental tissue proportions of the canine teeth belonging to the different *H. ergaster* and *H. erectus* populations. Likewise, new data about tissue proportion of the posterior

teeth belonging to Sima de los Huesos and Gran Dolina individuals could help to increase the amount of information available on the taxonomical distinctive patterns of these populations.

Acknowledgments

This study has been supported by the Dirección General de Investigación of the Spanish 'Ministerio de Economía y Competitividad' (MINECO/FEDER) grant number: CGL2015-65387-C3-1, 3-P. We also wish to acknowledge The Leakey Foundation for the personal support provided by Gordon Getty and Dub Crook to one of the authors (MM-T). CG-C and MM-M are funded by a doctoral grant financed by the European Social Funds through the 'Consejería de Educación, Junta de Castilla y León'. LM-F received financial support from the French State as part of the 'Investments for the future' Programme IdEx Bordeaux, reference ANR-10-IDEX-03-02. MMP is the recipient of a post-doctoral research grant at Atapuerca Foundation. Some of the micro-CT images were obtained in the Laboratory of Microscopy of the CENIEH-ICTS (Spain) in collaboration with CENIEH staff. The rest of the dental samples were scanned in the Multidisciplinary Laboratory of the International Centre for Theoretical Physics (ICTP) of Trieste in collaboration with Dr. Clément Zanolli and Claudio Tuniz. The African sample from Sudan was provided by Dr Christopher Dean from the Anatomy Department at University College, London. We are indebted to A. Oettlé, G. Krüger and E.N. L'Abbé for kindly authorizing access to the Pretoria Bone Collection (PBC) of the University of Pretoria, and to Dr. Clément Zanolli for interceding and making it possible. We also deeply thank F. de Beer and J. Hoffman for carrying out the X-ray micro-CT imaging of the human specimens from the PBC included in this study. In the same way we would like to acknowledge to Dr. Bernardo Perea-Pérez, for authorizing access to the Escuela de Medicinal Legal de Madrid Collection.

Appendix. Supplementary data

Supplementary data associated with this article can be found, in the online version, at https://doi.org/10.1016/j.crpv.2018.06.004.

References

Anton, S.C., 1990. Neandertals and the anterior dental loading hypothesis: a biomechanical evaluation of bite force production. Kroeber Anthropol. Soc. Pa 7, 67–76.

Arnold, L.J., Demuro, M., Parés, J.M., Arsuaga, J.L., Aranburu, A., Bermúdez de Castro, J.M., Carbonell, E., 2014. Luminescence dating and palaeomagnetic age constraint on hominins from Sima de los Huesos, Atapuerca, Spain. J. Hum. Evol. 67, 85–107, http://dx.doi.org/10.1016/j.jhevol.2013.12.001.

Arsuaga, J.L., 1993. Les hommes fossiles de la Sierra de Atapuerca. Rech. 260, 1399–1400, http://dx.doi.org/10.1038/362534a0.

Arsuaga, J.L., Carretero, J.-M., Lorenzo, C., Gómez-Olivencia, A., Pablos, A., Rodríguez, L., García-González, R., Bonmatí, A., Quam, R.M., Pantoja-Pérez, A., Martínez, I., Aranburu, A., Gracia-Téllez, A., Poza-Rey, E., Sala, N., García, N., Velasco, A.A. de, Cuenca-Bescós, G., Castro, J.M.B. de, Carbonell, E., 2015. Postcranial morphology of the Middle Pleistocene humans from Sima de los Huesos, Spain. Proc. Natl. Acad. Sci. USA 112, 11524–11529, http://dx.doi.org/10.1073/pnas.1514828112.

Arsuaga, J.L., Carretero, J.M., Martínez, I., Gracia, A., 1991. Cranial remains and long bones from Atapuerca/Ibeas (Spain). J. Hum. Evol. 20, 191–230, http://dx.doi.org/10.1016/0047-2484(91)90073-5.

Arsuaga, J.L., Martínez, I., Arnold, L.J., Aranburu, A., Gracia-Téllez, A., Sharp, W.D., Quam, R.M., Falguères, C., Pantoja-Pérez, A., Bischoff, J., Poza-Rey, E., Parés, J.M., Carretero, J.M., Demuro, M., Lorenzo, C., Sala, N., Martinón-Torres, M., García, N., Velasco, A.A. de, Cuenca-Bescós, G., Gómez-Olivencia, A., Moreno, D., Pablos, A., Shen, C.-C., Rodríguez, L., Ortega, A.I., García, R., Bonmatí, A., Castro, J.M.B. de, Carbonell, E., 2014. Neandertal roots: Cranial and chronological evidence from Sima de los Huesos. Science 344, 1358–1363, http://dx.doi.org/10.1126/science.1253958.

Arsuaga, J.L., Martínez, I., Gracia, A., Lorenzo, C., 1997. The Sima de los Huesos crania (Sierra de Atapuerca, Spain). A comparative study. J. Hum. Evol. 33, 219–281.

Bayle, P., Alcaraz, M., Zapata, J., Lombardi, V.A., Pérez-Pérez, A., Pinilla, B., Le Luyer, M., Robson Brown, K., Romero, A., Willman, J.-C., Lacy, S.A., Ortega, J., Karaková, K., 2017. The Palomas dental remains: Enamel thickness and tissues proportions. In: Trinkaus, E., Walker, M.J. (Eds.), The people of Palomas: Neandertals from the Sima de las Palomas del Cabezo Gordo, Southeastern Spain. Tex. AM Univ. Anthropol. Ser, pp. 115–137.

Bayle, P., Braga, J., Mazurier, A., Macchiarelli, R., 2009a. Dental developmental pattern of the Neanderthal child from Roc de Marsal: a high-resolution 3D analysis. J. Hum. Evol. 56, 66–75, http://dx.doi.org/10.1016/j.jhevol.2008.09.002.

Bayle, P., Braga, J., Mazurier, A., Macchiarelli, R., 2009b. Brief Communication: high-resolution assessment of the dental developmental pattern and characterization of tooth tissue proportions in the late Upper Paleolithic child from La Madeleine. France. Am. J. Phys. Anthropol. 138, 493–498, http://dx.doi.org/10.1002/ajpa.21000.

Bayle, P., Macchiarelli, R., Trinkaus, E., Duarte, C., Mazurier, A., Zilhão, J., 2010. Dental maturational sequence and dental tissue proportions in the early Upper Paleolithic child from Abrigo do Lagar Velho. Portugal. Proc. Natl. Acad. Sci. USA 107, 1338–1342, http://dx.doi.org/10.1073/pnas.0914202107.

Benazzi, S., Panetta, D., Fornai, C., Toussaint, M., Gruppioni, G., Hublin, J.-J., 2014. Technical note: guidelines for the digital computation of 2D and 3D enamel thickness in hominoid teeth. Am. J. Phys. Anthropol. 153, 305–313, http://dx.doi.org/10.1002/ajpa.22421.

Benazzi, S., Viola, B., Kullmer, O., Fiorenza, L., Harvati, K., Paul, T., Gruppioni, G., Weber, G.W., Mallegni, F., 2011. A reassessment of the Neanderthal teeth from Taddeo cave (southern Italy). J. Hum. Evol. 61, 377–387, http://dx.doi.org/10.1016/j.jhevol.2011.05.001.

Berger, G.W., Pérez-González, A., Carbonell, E., Arsuaga, J.L., Bermúdez de Castro, J.M., Ku, T.-L., 2008. Luminescence chronology of cave sediments at the Atapuerca paleoanthropological site, Spain. J. Hum. Evol. 55, 300–311, http://dx.doi.org/10.1016/j.jhevol.2008.02.012.

Bermúdez de Castro, J.M., 1986. Dental remains from Atapuerca (Spain) I, Metrics. J. Hum. Evol. 15, 265–287, http://dx.doi.org/10.1016/S0047-2484(86)80054-9.

Bermúdez de Castro, J.M., Arsuaga, J.L., Carbonell, E., Rosas, A., Martínez, I., Mosquera, M., 1997. A hominid from the lower Pleistocene of Atapuerca, Spain: possible ancestor to Neandertals and modern humans. Science 276, 1392–1395.

Bermúdez de Castro, J.M., Martinón-Torres, M., Arsuaga, J.L., Carbonell, E., 2017. Twentieth anniversary of *Homo antecessor* (1997–2017): a review. Evol. Anthropol. 26, 157–171, http://dx.doi.org/10.1002/evan.21540.

Bermúdez de Castro, J.M., Martinón-Torres, M., Blasco, R., Rosell, J., Carbonell, E., 2013. Continuity or discontinuity in the European early Pleistocene human settlement: the Atapuerca evidence. Quat. Sci. Rev. 76, 53–65, http://dx.doi.org/10.1016/j.quascirev.2013.06.023.

Bermúdez de Castro, J.M., Martinón-Torres, M., Carbonell, E., Sarmiento, S., Rosas, A., van der Made, J., Lozano, M., 2004. The Atapuerca sites and their contribution to the knowledge of human evolution in Europe. Evol. Anthropol. 13, 25–41, http://dx.doi.org/10.1002/evan.10130.

Bermúdez de Castro, J.M., Martinón-Torres, M., Martínez de Pinillos, M., García-Campos, C., Modesto-Mata, M., Martín-Francés, L., Arsuaga, J.L., 2018. Metric and morphological comparison between the Arago (France) and Atapuerca-Sima de los Huesos (Spain) dental samples, and the origin of Neanderthals. Quat. Sci. Rev., http://dx.doi.org/10.1016/j.quascirev.2018.04.003.

Bermúdez de Castro, J.M., Martinón-Torres, M., Martín-Francés, L., Modesto-Mata, M., Martínez-de-Pinillos, M., García, C., Carbonell, E., 2015. *Homo antecessor*: the state of the art eighteen years later. Quat. Int., http://dx.doi.org/10.1016/j.quaint.2015.03.049.

Bermúdez de Castro, J.M., Martinón-Torres, M., Sarmiento, S., Lozano, M., 2003. Gran Dolina-TD6 versus Sima de los Huesos dental

samples from Atapuerca: evidence of discontinuity in the European Pleistocene population? J. Archaeol. Sci. 30, 1421–1428, http://dx.doi.org/10.1016/S0305-4403(03)00036-0.
Bermúdez de Castro, J.M., Pérez-González, A., Martinón-Torres, M., Gómez-Robles, A., Rosell, J., Prado, L., Sarmiento, S., Carbonell, E., 2008. A new early Pleistocene hominin mandible from Atapuerca-TD6, Spain. J. Hum. Evol. 55, 729–735, http://dx.doi.org/10.1016/j.jhevol.2008.03.006.
Bermúdez de Castro, J.M., Rosas, A., Nicolás, M.E., 1999a. Dental remains from Atapuerca-TD6 (Gran Dolina site, Burgos, Spain). J. Hum. Evol. 37, 523–566, http://dx.doi.org/10.1006/jhev.1999.0323.
Beynon, A.D., Wood, B.A., 1986. Variations in enamel thickness and structure in East African hominids. Am. J. Phys. Anthropol. 70, 177–193, http://dx.doi.org/10.1002/ajpa.1330700205.
Bischoff, J.L., Shamp, D.D., Aramburu, A., Arsuaga, J.L., Carbonell, E., Bermúdez de Castro, J.M., 2003. The Sima de los Huesos hominids date to beyond U/Th equilibrium (>350 kyr) and perhaps to 400-500 kyr: new radiometric dates. J. Archaeol. Sci. 30, 275–280, http://dx.doi.org/10.1006/jasc.2002.0834.
Brace, C.L., 1979. Krapina, classic Neanderthals, and the evolution of the European face. J. Hum. Evol. 8, 527–550.
Buti, L., Le Cabec, A., Panetta, D., Tripodi, M., Salvadori, P.A., Hublin, J.-J., Feeney, R.N.M., Benazzi, S., 2017. 3D enamel thickness in Neandertal and modern human permanent canines. J. Hum. Evol. 113, 162–172, http://dx.doi.org/10.1016/j.jhevol.2017.08.009.
Carbonell, E., Bermúdez de Castro, J.M., Arsuaga, J.L., Díez Fernández-Lomana, J.C., Rosas, A., Cuenca-Bescos, G., Sala, R., Mosquera, M., Rodríguez, X.P., 1995. Lower Pleistocene hominids and artifacts from Atapuerca-TD6 (Spain). Science 269, 826–830, http://dx.doi.org/10.1126/science.7638598.
Constantino, P.J., Lee, J.J.-W., Morris, D., Lucas, P.W., Hartstone-Rose, A., Lee, W.-K., Dominy, N.J., Cunningham, A., Wagner, M., Lawn, B.R., 2011. Adaptation to hard-object feeding in sea otters and hominins. J. Hum. Evol. 61, 89–96, http://dx.doi.org/10.1016/j.jhevol.2011.02.009.
Dean, C., 2009. Extension rates and growth in tooth height of modern human and fossil hominin canines and molars. Front. Oral Biol. 13, 68–73, http://dx.doi.org/10.1159/000242394.
Dean, C., Leakey, M.G., Reid, D., Schrenk, F., Schwartz, G.T., Stringer, C., Walker, A., 2001. Growth processes in teeth distinguish modern humans from *Homo erectus* and earlier hominins. Nature 414, 628–631, http://dx.doi.org/10.1038/414628a.
Dumont, E.R., 1995. Enamel thickness and dietary adaptation among extant primates and chiropterans. J. Mammal. 76, 1127–1136.
Duval, M., Grün, R., Parés, J.M., Martín-Francés, L., Campaña, I., Rosell, J., Shao, Q., Arsuaga, J.L., Carbonell, E., Bermúdez de Castro, J.M., 2018. The first direct ESR analysis of a hominin tooth from Atapuerca Gran Dolina TD-6 (Spain) supports the antiquity of *Homo antecessor*. Quat. Geochron., http://dx.doi.org/10.1016/j.quageo.2018.05.001.
Elamin, F., Liversidge, H.M., 2013. Malnutrition has no effect on the timing of human tooth formation. Plos One 8, e72274, http://dx.doi.org/10.1371/journal.pone.0072274.
Falguères, C., Bahain, J.-J., Yokoyama, Y., Arsuaga, J.L., Bermudez de Castro, J.M., Carbonell, E., Bischoff, J.L., Dolo, J.-M., 1999. Earliest humans in Europe: the age of TD6 Gran Dolina, Atapuerca, Spain. J. Hum. Evol. 37, 343–352, http://dx.doi.org/10.1006/jhev.1999.0326.
Feeney, R.N., Zermeno, J.P., Reid, D.J., Nakashima, S., Sano, H., Bahar, A., Hirosh, S., Armasastra, B., Hublin, J.-J., Smith, T.M., 2010. Enamel thickness in Asian human canines and premolars. Anthropol. Sci. 118, 191–198.
García-Campos, C., Martinón-Torres, M., Martín-Francés, L., Martínez de Pinillos, M., Modesto-Mata, M., Perea-Pérez, B., Zanolli, C., Labajo González, E., Sánchez Sánchez, J.A., Ruiz Mediavilla, E., Tuniz, C., Bermúdez de Castro, J.M., 2018. Contribution of dental tissues to sex determination in modern human populations. Am. J. Phys. Anthropol. 166, 459–547, http://dx.doi.org/10.1002/ajpa.23447.
Giustina, A., Veldhuis, J.D., 1998. Pathophysiology of the neuroregulation of growth hormone secretion in experimental animals and the human. Endocr. Rev. 19, 717–797, http://dx.doi.org/10.1210/edrv.19.6.0353.
Goldberg, M., Kulkarni, A.B., Young, M., Boskey, A., 2011. Dentin: structure, composition and mineralization. Front. Biosci. Elite Ed. 3, 711–735.
Gómez-Robles, A., 2010. Análisis de la forma dental en la filogenia humana. Tendencias y modelos evolutivos basados en métodos de morfometría geométrica (PhD dissertation). Universidad de Granada.
Gómez-Robles, A., Bermúdez de Castro, J.M., Martinón-Torres, M., Prado-Simón, L., Arsuaga, J.L., 2012. A geometric morphometric analysis of hominin upper second and third molars, with particular emphasis on European Pleistocene populations. J. Hum. Evol. 63, 512–526, http://dx.doi.org/10.1016/j.jhevol.2012.06.002.
Gómez-Robles, A., Martinón-Torres, M., Bermúdez de Castro, J.M., Margvelashvili, A., Bastir, M., Arsuaga, J.L., Pérez-Pérez, A., Estebaranz, F., Martínez, L.M., 2007. A geometric morphometric analysis of hominin upper first molar shape. J. Hum. Evol. 53, 272–285, http://dx.doi.org/10.1016/j.jhevol.2007.02.002.
Gómez-Robles, A., Martinón-Torres, M., Bermúdez de Castro, J.M., Prado, L., Sarmiento, S., Arsuaga, J.L., 2008. Geometric morphometric analysis of the crown morphology of the lower first premolar of hominins, with special attention to Pleistocene *Homo*. J. Hum. Evol. 55, 627–638, http://dx.doi.org/10.1016/j.jhevol.2008.03.011.
Gómez-Robles, A., Martinón-Torres, M., Bermúdez de Castro, J.M., Prado-Simón, L., Arsuaga, J.L., 2011. A geometric morphometric analysis of hominin upper premolars. Shape variation and morphological integration. J. Hum. Evol. 61, 688–702, http://dx.doi.org/10.1016/j.jhevol.2011.09.004.
Grine, F.E., 2002. Scaling of tooth enamel thickness, and molar crown size reduction in modern humans. S. Afr. J. Sci. 98, 503–509.
Grine, F.E., 2005. Enamel thickness of deciduous and permanent molars in modern *Homo sapiens*. Am. J. Phys. Anthropol. 126, 14–31, http://dx.doi.org/10.1002/ajpa.10277.
Grine, F.E., Martin, L.B., 1988. Enamel thickness and development in *Australopithecus* and *Paranthropus*. In: Grine, F.E. (Ed.), The evolutionary history of the "robust" australopithecines. Aldine de Gruyter, New York, pp. 3–42.
Hall, K.R.L., Schaller, G.B., 1964. Tool-using behavior of the California sea otter. J. Mammal. 45, 287–298, http://dx.doi.org/10.2307/1376994.
Harvati, K., Singh, N., López, E.N., 2011. A three-dimensional look at the Neanderthal mandible. In: Condemi, S., Weniger, G.C. (Eds.), Continuity and discontinuity in the peopling of Europe. Vertebrate Paleobiology and Paleoanthropology Series. Springer, Dordrecht, pp. 179–192.
Hinton, R.J., 1981. Form and patterning of anterior tooth wear among aboriginal human groups. Am. J. Phys. Anthropol. 54, 555–564, http://dx.doi.org/10.1002/ajpa.1330540409.
Hublin, J.-J., 1998. Climate change, paleogeography and the evolution of the Neandertals. In: Akazawa, T., Aoki, K., Bar-Yosef, O. (Eds.), Neandertals and modern humans in Western Asia. Plenum Publishing, New York, pp. 295–310.
Irish, J.D., 1998. Ancestral dental traits in recent Sub-Saharan Africans and the origins of modern humans. J. Hum. Evol. 34, 81–98, http://dx.doi.org/10.1006/jhev.1997.0191.
Kono, R.T., 2004. Molar enamel thickness and distribution patterns in extant great apes and humans: new insights based on a 3-dimensional whole crown perspective. Anthropol. Sci. 112, 121–146, http://dx.doi.org/10.1537/ase.03106.
Kono, R.T., Suwa, G., 2008. Enamel distribution patterns of extant human and hominoid molars: occlusal versus lateral enamel thickness. Bull. Natl. Mus. Nat. Sci. Ser D 34, 1–9.
Kono, R.T., Suwa, G., Tanijiri, T., 2002. A three-dimensional analysis of enamel distribution patterns in human permanent first molars. Arch. Oral Biol. 47, 867–875, http://dx.doi.org/10.1016/S0003-9969(02)00151-6.
Kupczik, K., Hublin, J.-J., 2010. Mandibular molar root morphology in Neanderthals and Late Pleistocene and recent *Homo sapiens*. J. Hum. Evol. 59, 525–541, http://dx.doi.org/10.1016/j.jhevol.2010.05.009.
L'Abbé, E.N., Loots, M., Meiring, J.H., 2005. The Pretoria Bone Collection: a modern South African skeletal sample. HOMO J. Comp. Hum. Biol. 56, 197–205, http://dx.doi.org/10.1016/j.jchb.2004.10.004.
Le Cabec, A., Gunz, P., Kupczik, K., Braga, J., Hublin, J.-J., 2013. Anterior tooth root morphology and size in Neanderthals: taxonomic and functional implications. J. Hum. Evol. 64, 169–193, http://dx.doi.org/10.1016/j.jhevol.2012.08.011.
Le Cabec, A., Kupczik, K., Gunz, P., Braga, J., Hublin, J.-J., 2012. Long anterior mandibular tooth roots in Neanderthals are not the result of their large jaws. J. Hum. Evol. 63, 667–681, http://dx.doi.org/10.1016/j.jhevol.2012.07.003.
Lieberman, D.E., 2011. Evolution of the human head. Harvard University Press, Cambridge, MA, USA.
Lucas, P., Constantino, P., Wood, B., Lawn, B., 2008. Dental enamel as a dietary indicator in mammals. BioEss. 30, 374–385, http://dx.doi.org/10.1002/bies.20729.
Martin, L.B., 1985. Significance of enamel thickness in hominid evolution. Nature 314, 260–263.
Martin, L.B., 1983. The relationships of the later Miocene Hominoidea. (PhD dissertation). University of London, London.
Martin, L.B., Olejniczak, A.J., Maas, M.C., 2003. Enamel thickness and microstructure in pitheciin primates, with comments on dietary adaptations of the middle Miocene hominoid *Kenyapithecus*. J. Hum. Evol. 45, 351–367, http://dx.doi.org/10.1016/j.jhevol.2003.08.005.

Martínez, I., Arsuaga, J.L., 1997. The temporal bones from Sima de los Huesos Middle Pleistocene site (Sierra de Atapuerca, Spain). A phylogenetic approach. J. Hum. Evol. 33, 283–318, http://dx.doi.org/10.1006/jhev.1997.0155.

Martínez de Pinillos, M., Martinón-Torres, M., Skinner, M.M., Arsuaga, J.L., García-Téllez, A., Martínez, I., Martín-Francés, L., Bermúdez de Castro, J.M., 2014. Trigonid crests expression in Atapuerca-Sima de los Huesos lower molars: internal and external morphological expression and evolutionary inferences. C.R. Palevol 13, 205–221, http://dx.doi.org/10.1016/j.crpv.2013.10.008.

Martinón-Torres, M., Bermúdez de Castro, J.M., Gómez-Robles, A., Margvelashvili, A., Prado, L., Lordkipanidze, D., Vekua, A., 2008. Dental remains from Dmanisi (Republic of Georgia): morphological analysis and comparative study. J. Hum. Evol. 55, 249–273, http://dx.doi.org/10.1016/j.jhevol.2007.12.008.

Martinón-Torres, M., Bermúdez de Castro, J.M., Gómez-Robles, A., Prado-Simón, L., Arsuaga, J.L., 2012. Morphological description and comparison of the dental remains from Atapuerca-Sima de los Huesos site (Spain). J. Hum. Evol. 62, 7–58, http://dx.doi.org/10.1016/j.jhevol.2011.08.007.

Martinón-Torres, M., Martínez de Pinillos, M., Skinner, M.M., Martín-Francés, L., Gracia-Téllez, A., Martínez, I., Arsuaga, J.L., Bermúdez de Castro, J.M., 2014. Talonid crests expression at the enamel-dentine junction of hominin lower permanent and deciduous molars. C.R. Palevol 13, 223–234, http://dx.doi.org/10.1016/j.crpv.2013.12.002.

Meyer, M., Arsuaga, J.L., de Filippo, C., Nagel, S., Aximu-Petri, A., Nickel, B., Martínez, I., Gracia, A., de Castro, J.M.B., Carbonell, E., Viola, B., Kelso, J., Prüfer, K., Pääbo, S., 2016. Nuclear DNA sequences from the Middle Pleistocene Sima de los Huesos hominins. Nature 531, 504–507, http://dx.doi.org/10.1038/nature17405.

Molnar, S., 1971. Human tooth wear, tooth function and cultural variability. Am. J. Phys. Anthropol. 34, 175–189, http://dx.doi.org/10.1002/ajpa.1330340204.

Moreno, D., Falguères, C., Pérez-González, A., Voinchet, P., Ghaleb, B., Despriée, J., Bahain, J.-J., Sala, R., Carbonell, E., Bermúdez de Castro, J.M., Arsuaga, J.L., 2015. New radiometric dates on the lowest stratigraphical section (TD1 to TD6) of Gran Dolina site (Atapuerca, Spain). Quat. Geochron. 30, 535–540, http://dx.doi.org/10.1016/j.quageo.2015.05.007.

Nishiyama, K., Sugimoto, T., Kaji, H., Kanatani, M., Kobayashi, T., Chihara, K., 1996. Stimulatory effect of growth hormone on bone resorption and osteoclast differentiation. Endocrin. 137, 35–41, http://dx.doi.org/10.1210/endo.137.1.8536635.

Olejniczak, A.J., Gilbert, C.C., Martin, L.B., Smith, T.M., Ulhaas, L., Grine, F.E., 2007. Morphology of the enamel-dentine junction in sections of anthropoid primate maxillary molars. J. Hum. Evol. 53, 292–301.

Olejniczak, A.J., Smith, T.M., Feeney, R.N.M., Macchiarelli, R., Mazurier, A., Bondioli, L., Rosas, A., Fortea, J., de la Rasilla, M., Garcia-Tabernero, A., Radovcić, J., Skinner, M.M., Toussaint, M., Hublin, J.-J., 2008a. Dental tissue proportions and enamel thickness in Neandertal and modern human molars. J. Hum. Evol. 55, 12–23, http://dx.doi.org/10.1016/j.jhevol.2007.11.004.

Olejniczak, A.J., Tafforeau, P., Feeney, R.N.M., Martin, L.B., 2008b. Three-dimensional primate molar enamel thickness. J. Hum. Evol. 54, 187–195, http://dx.doi.org/10.1016/j.jhevol.2007.09.014.

Pablos, A., Lorenzo, C., Martínez, I., Bermúdez de Castro, J.M., Martinón-Torres, M., Carbonell, E., Arsuaga, J.L., 2012. New foot remains from the Gran Dolina-TD6 Early Pleistocene site (Sierra de Atapuerca, Burgos, Spain). J. Hum. Evol. 63, 610–623, http://dx.doi.org/10.1016/j.jhevol.2012.06.008.

Pablos, A., Pantoja-Pérez, A., Martínez, I., Lorenzo, C., Arsuaga, J.L., 2017. Metric and morphological analysis of the foot in the Middle Pleistocene sample of Sima de los Huesos (Sierra de Atapuerca, Burgos, Spain). Quat. Int. 433, 103–113, http://dx.doi.org/10.1016/j.quaint.2015.08.044.

Plavcan, J.M., 2012. Sexual size dimorphism, canine dimorphism, and male-male competition in primates: where do humans fit in? Hum. Nat. 23, 45–67, http://dx.doi.org/10.1007/s12110-012-9130-3.

Ramirez Rozzi, F., 1998. Can enamel microstructure be used to establish the presence of different species of Plio-Pleistocene hominids from Omo, Ethiopia? J. Hum. Evol. 35, 543–576.

Rathmann, H., Reyes-Centeno, H., Ghirotto, S., Creanza, N., Hanihara, T., Harvati, K., 2017. Reconstructing human population history from dental phenotypes. Sci. Rep. 7, 12495, http://dx.doi.org/10.1038/s41598-017-12621-y.

Rink, W.J., Schwarcz, H.P., Smith, F.H., Radovčić, J., 1995. ESR ages for Krapina hominids. Nature 378, 24.

Rosas, A., Bermúdez de Castro, J.M., 1999. The ATD6-5 mandibular specimen from Gran Dolina (Atapuerca, Spain). Morphological study and phylogenetic implications. J. Hum. Evol. 37, 567–590, http://dx.doi.org/10.1006/jhev.1999.0340.

Saunders, S.R., Chan, A.H.W., Kahlon, B., Kluge, H.F., FitzGerald, C.M., 2007. Sexual dimorphism of the dental tissues in human permanent mandibular canines and third premolars. Am. J. Phys. Anthropol. 133, 735–740, http://dx.doi.org/10.1002/ajpa.20553.

Schwartz, G.T., 2000. Taxonomic and functional aspects of the patterning of enamel thickness distribution in extant large-bodied hominoids. Am. J. Phys. Anthropol. 111, 221–244, https://doi.org/10.1002/(SICI)1096–8644(200002)111:2<221::AID-AJPA8>3.0.CO;2-G.

Schwartz, G.T., Dean, M.C., 2005. Sexual dimorphism in modern human permanent teeth. Am. J. Phys. Anthropol. 128, 312–317, http://dx.doi.org/10.1002/ajpa.20211.

Scott, G.R., Turner, C.G., 2000. The anthropology of modern human teeth: Dental morphology and its variation in recent human populations. Cambridge University Press, Cambridge.

Skinner, M.M., Alemseged, Z., Gaunitz, C., Hublin, J.-J., 2015. Enamel thickness trends in Plio-Pleistocene hominin mandibular molars. J. Hum. Evol. 85, 35–45, http://dx.doi.org/10.1016/j.jhevol.2015.03.012.

Skinner, M.M., Gunz, P., Wood, B.A., Hublin, J.-J., 2008a. Enamel-dentine junction (EDJ) morphology distinguishes the lower molars of *Australopithecus africanus* and *Paranthropus robustus*. J. Hum. Evol. 55, 979–988.

Skinner, M.M., Wood, B.A., Boesch, C., Olejniczak, A.J., Rosas, A., Smith, T.M., Hublin, J.-J., 2008b. Dental trait expression at the enamel-dentine junction of lower molars in extant and fossil hominoids. J. Hum. Evol. 54, 173–186, http://dx.doi.org/10.1016/j.jhevol.2007.09.012.

Slootweg, M.C., 1993. Growth hormone and bone. Horm. Metab. Res. 25, 335–343, http://dx.doi.org/10.1055/s-2007-1002115.

Smith, T.M., Olejniczak, A.J., Kupczik, K., Lazzari, V., Vos, J., Kullmer, O., Schrenk, F., Hublin, J.-J., Jacob, T., Tafforeau, P., 2009. Taxonomic assessment of the Trinil molars using non-destructive 3D structural and developmental analysis. PaleoAnthropol. 2009, 117–129.

Smith, T.M., Olejniczak, A.J., Martin, L.B., Reid, D.J., 2005. Variation in hominoid molar enamel thickness. J. Hum. Evol. 48, 575–592, http://dx.doi.org/10.1016/j.jhevol.2005.02.004.

Smith, T.M., Olejniczak, A.J., Reh, S., Reid, D.J., Hublin, J.-J., 2008. Brief Communication: enamel thickness trends in the dental arcade of humans and chimpanzees. Am. J. Phys. Anthropol. 136, 237–241, http://dx.doi.org/10.1002/ajpa.20796.

Smith, T.M., Olejniczak, A.J., Reid, D.J., Ferrell, R.J., Hublin, J.J., 2006. Modern human molar enamel thickness and enamel-dentine junction shape. Arch. Oral Biol. 51, 974–995, http://dx.doi.org/10.1016/j.archoralbio.2006.04.012.

Smith, T.M., Olejniczak, A.J., Zermeno, J.P., Tafforeau, P., Skinner, M.M., Hoffmann, A., Radovčić, J., Toussaint, M., Kruszynski, R., Menter, C., Moggi-Cecchi, J., Glasmacher, U.A., Kullmer, O., Schrenk, F., Stringer, C., Hublin, J.-J., 2012. Variation in enamel thickness within the genus *Homo*. J. Hum. Evol. 62, 395–411, http://dx.doi.org/10.1016/j.jhevol.2011.12.004.

Tafforeau, P., 2004. Phylogenetic and functional aspects of tooth enamel microstructure and three-dimensional structure of modern and fossil primate molars: Contributions of X-ray synchrotron microtomography. (PhD dissertation). Université de Montpellier II, Montpellier.

Trinkaus, E., 1987. The Neandertal face: evolutionary and functional perspectives on a recent hominid face. J. Hum. Evol. 16, 429–443, http://dx.doi.org/10.1016/0047-2484(87)90071-6.

Tuniz, C., Bernardini, F., Cicuttin, A., Crespo, M.L., Dreossi, D., Gianoncelli, A., Mancini, L., Mendoza Cuevas, A., Sodini, N., Tromba, G., Zanini, F., Zanolli, C., 2013. The ICTP-Elettra X-ray laboratory for cultural heritage and archaeology. Nucl. Instrum. Methods Phys. Res. Sect. Accel. Spectrometers Detect. Assoc. Equip. 711, 106–110, http://dx.doi.org/10.1016/j.nima.2013.01.046.

Wolpoff, M.H., 1979. The Krapina dental remains. Am. J. Phys. Anthropol. 50, 67–113, http://dx.doi.org/10.1002/ajpa.1330500110.

Wolpoff, M.H., 1999. Paleoanthropology, 2nd ed. McGraw-Hill, Boston.

Young, W.G., Zhang, C.Z., Li, H., Osborne, P., Waters, M.J., 1992. The influence of growth hormone on cell proliferation in odontogenic epithelia by bromodeoxyuridine immunocytochemistry and morphometry in the Lewis dwarf rat. J. Dent. Res. 71, 1807–1811.

Zanolli, C., 2014. Molar crown inner structural organization in Javanese *Homo erectus*. Am. J. Phys. Anthropol. 156, 148–157, http://dx.doi.org/10.1002/ajpa.22611.

Zanolli, C., Bondioli, L., Coppa, A., Dean, M.C., Bayle, P., Candilio, F., Capuani, S., Dreossi, D., Fiore, I., Frayer, D.W., Libsekal, Y., Mancini, L., Rook, L., Medin Tekle, T., Tuniz, C., Macchiarelli, R., 2014. The late Early Pleistocene human dental remains from Uadi Aalad and

Mulhuli-Amo (Buia), Eritrean Danakil: macromorphology and microstructure. J. Hum. Evol. 74, 96–113.

Zanolli, C., Mazurier, A., 2013. Endostructural characterization of the *H. heidelbergensis* dental remains from the early Middle Pleistocene site of Tighenif. Algeria. C.R. Palevol 12, 293–304, http://dx.doi.org/10.1016/j.crpv.2013.06.004.

Zanolli, C., Pan, L., Dumoncel, J., Kullmer, O., Kundrát, M., Liu, W., Macchiarelli, R., Mancini, L., Schrenk, F., Tuniz, C., 2018. Inner tooth morphology of *Homo erectus* from Zhoukoudian. New evidence from an old collection housed at Uppsala University. Sweden. J. Hum. Evol. 116, 1–13, http://dx.doi.org/10.1016/j.jhevol.2017.11.002.